In-situ determination of Nd isotope ratios in apatite by LA-MC-ICPMS: Challenges and limitations

Régis Doucelance, Emilie Bruand, Simon Matte, Chantal Bosq, Delphine Auclair, Abdelmouhcine Gannoun

In-situ determination of Nd isotope ratios in apatite by LA-MC-ICPMS: challenges and limitations

Régis DOUCELANCE, Emilie BRUAND, Simon MATTE, Chantal BOSQ, Delphine AUCLAIR, and Abdel-Mouhcine GANNOUN

Laboratoire Magmas et Volcans, CNRS UMR 6524, Université Clermont Auvergne, F-63000 Clermont-Ferrand, France.

Abstract

In-situ measurement of Sm-Nd isotopes in rare-earth-element bearing minerals has been successfully used in the recent years to access the history of old Earth materials (e.g. Hammerli *et al.*, 2019; Fisher *et al.*, 2020). However, the analytical protocol of Laser Ablation-Multi Collector-Inductively Coupled Plasma Mass Spectrometry (LA-MC-ICPMS) for Sm-Nd measurements strongly depends on the instruments, the analytical parameters and the applied corrections. In this paper, we intend to summarize some of the difficulties to set up this technique. We present new results by evaluating the influence of laser parameters (spot size, fluence, frequency and He/N_2 gas flows) on $^{143}Nd/^{144}Nd$, $^{145}Nd/^{144}Nd$ and $^{147}Sm/^{144}Nd$ ratios. We also report results on tests of cone geometry and interference and mass discrimination corrections on both the accuracy and precision of Nd isotopic analyzes. We report new Sm-Nd measurements performed by TIMS and LA-MC-ICPMS on Durango reference apatite (Mexico) and apatite crystals from 2 carbonatites (Fogo, Cape Verde and Phalaborwa, South Africa). We conclude from these measurements that the laser parameters have no influence on the $^{143}Nd/^{144}Nd$ and $^{145}Nd/^{144}Nd$ isotopic ratios. The value of the $^{147}Sm/^{144}Nd$ ratio, however, is correlated to the size of the spot (Fisher *et al.*, 2020). More importantly, we show that $^{147}Sm/^{144}Nd$ ratio measurements can vary when the He/N_2 gas flows are changed even punctually (e.g. sample exchange) during an analytical session and decrease systematically during the day, which we relate to a systematic instrumental drift. We also conclude that our Durango crystal is homogeneous for Nd isotopic ratios, and slightly heterogeneous for Sm/Nd at the level of ±1-1.5% allowing accurate measurements when used as external standard. We retrieve expected isotopic ratios for both recent Fogo (4 Ma old) and ancient Phalaborwa (2060 Ma old) samples and we achieve precisions in the order of 125-150 ppm (1.3-1.5 εNd-units) for the $^{143}Nd/^{144}Nd$ ratio for a laser spot of 40 µm, which can be considered as a reasonable size for apatite crystals in most geological samples. Finally, we present raster measurements allowing to improve the precision by a factor of ~2 with 70 ppm (0.7 εNd-units).

Keywords : Nd, isotopes, in-situ, analysis, LA-MC-ICPMS, apatite

---

1. Introduction

The Samarium-Neodymium (Sm-Nd) isotopic systematics relies on the radioactive decay of the long-lived ^{147}Sm isotope to the radiogenic ^{143}Nd (half-life of 106 ± 0.8 Gyr; Lugmair and Marti, 1978). Its application as a source tracer and/or a chronometer covers a wide range of geological subjects related to the differentiation and history of the Earth and other planets. The Sm-Nd pair involves two elements of the same family, the rare earth elements (REE), with a similar ionic radius, thus giving them similar chemical behaviors during magmatic processes. The small fractionation resulting from these characteristics and the long half-life of ^{147}Sm lead to relatively small variations of the Nd isotopic compositions with time. As a consequence, the ^{147}Sm-^{143}Nd systematics does not allow to determine ages of young rocks with a great precision. However, the possibly low chemical disturbance of the Sm-Nd pair during alteration and low degree of metamorphism can allow to minimize any post-magmatic events. The Sm-Nd isotopic systematics is therefore a powerful source tracer for old and possibly altered, geological samples.

The Nd isotopic ratios are classically determined on bulk rocks and/or mineral separates by thermal ionization (TIMS) or plasma source mass spectrometry (MC-ICPMS), after acid digestion of the samples and chemical separation of Nd from the other elements by ion-exchange resin chromatography. However, in-situ measurements are also possible by coupling the MC-ICPMS instrumentation to a laser ablation system (LA-MC-ICPMS; e.g. Foster and Vance, 2006; McFarlane and McCulloch, 2007; Fisher *et al.*, 2011; Mitchell *et al.*, 2011; Iizuka *et al.*, 2011; Yang *et al.*, 2014; Qian and Zhang, 2019; Fisher *et al.*, 2020; and references therein). In this case, the determination of the isotopic compositions is quicker, being free from the steps of dissolution and chemical separation. More importantly, it gives the possibility of considering much finer scales of heterogeneity than bulk-rock analyzes, at the level of a few tens of micrometers.

The in-situ measurement of isotopic compositions of Nd is suitable in minerals rich in this element (e.g. monazite, titanite, apatite). Apatite is an ideal candidate as its Nd concentrations are generally greater than several hundreds of ppm, and it is an ubiquitous phase in most rocks (magmatic, metamorphic and sedimentary), giving wide field of application in geology. Several laboratories have already developed the in-situ analysis of Nd isotopic ratios in this mineral. Analytical protocols are nearly similar at some extent, but diverge on other points such as correction for instrumental Sm-Nd fractionation (Fisher *et al.*, 2011; Iizuka *et al.*, 2011). Moreover, the accuracy and precision of isotopic measurements seem to be strongly dependent on the instrumentation used (laser system + MC-ICPMS), as well as the number and diversity of isotopic ratios analyzed on, leading to the necessity for each laboratory to justify for its own protocol. Here, we present new Sm-Nd results acquired on the Thermo Fisher Scientific™ Neptune Plus™ instrument at the Laboratoire Magmas et Volcans (LMV), Clermont-Ferrand, France, on apatite crystals from three different localities (Durango apatite and two carbonatite apatites). We detail the different corrections needed to obtain accurate and precise Nd isotopic ratios with a focus on the laser (size of the spot, fluence, frequency and He/N_2 gas flows) and MC-ICPMS parameters (*X* vs. *H* skimmer cones) and their influence on the measurements. From a more general point of view, this contribution aims to help geochemical laboratories to set up and implement an in-situ analysis protocol for Nd isotope ratios.

2. Durango and Phalaborwa apatites

Durango apatite is a fluorapatite (usually millimeter- to centimeter in size) which has been sampled from the Cerro de Mercado mine, Mexico. Its age is estimated to be 31.02 ± 0.22 Ma (U-Th-He thermochronology; McDowell *et al.*, 2005); it originated from hydrothermal processes in relation with Oligocene alkaline volcanic rocks (Lyons, 1988). Durango apatite is classically used as a reference standard for isotopic analysis of Nd by LA-MC-ICPMS (e.g. Foster and Vance, 2006; Fisher *et al.*, 2011; Yang *et al.*, 2014), and as a reference standard for halogens in microprobe analysis (Rønsbo, 1989; Hammouda *et al.*, 2010), for (U-Th)/He and fission track dating (Carlson and Lugmair, 1979; Zeitler *et al.*, 1987; Hasebe *et al.*, 2004; McDowell *et al.*, 2005; Flowers *et al.*, 2009), and for trace element analysis (e.g. Trotter and Eggins, 2006; Bruand *et al.*, 2014).

Using Durango apatite as a standard has several advantages: 1) it is present in large quantities in the form of multi-centimeter crystals, 2) it is relatively easy to obtain, and 3) it has been reported as homogeneous in Nd isotopes at the crystal scale with a restricted range of $^{143}Nd/^{144}Nd$ between 0.512434 and 0.512498 (Foster and Vance, 2006; Fisher *et al.*, 2011; Yang *et al.*, 2014; Xu *et al.*, 2018). Punctually, some studies have highlighted compositional variations between different Durango apatite crystals (e.g. Fisher *et al.*, 2011; Yang *et al.*, 2014). Thus, we tested the chemical and isotopic characteristics of the crystal studied in this contribution (sample #144954-4, Smithsonian National Museum of Natural History). For this purpose, three fragments of the mineral, weighting each between 10 and 20 mg and respectively called D1, D2 and D3, were cleaned with milliQ water to remove any dust on their surfaces and then acid-digested in Teflon vessel (savillex©) with a mixture of HNO_3-HF followed by HNO_3-$HClO_4$. Aliquots of around 5% of the digestions were used for Sm and Nd content measurements on an Agilent 7500C ICPMS instrument, whereas aliquots between 10 and 20% were mixed with a ^{150}Nd-^{149}Sm spike and passed through TRU- and Ln-Spec columns in order to determine their isotopic and chemical ratios ($^{143}Nd/^{144}Nd$, $^{145}Nd/^{144}Nd$ and $^{147}Sm/^{144}Nd$) by isotope dilution on a Thermo Electron™ Finnigan Triton™ thermo-ionization mass spectrometer (TIMS). All TIMS measurements were made in static mode with relay matrix rotation (also called the virtual amplifier) and double Re filaments. Isotope ratios were mass-fractionation corrected with $^{146}Nd/^{144}Nd = 0.7219$ and normalized to $^{143}Nd/^{144}Nd = 0.512100$ for the JNDi-1 Nd standard (Garçon *et al.*, 2018). Isotope dilution also assumed $^{150}Nd/^{144}Nd = 0.236451$, $^{149}Sm/^{147}Sm = 0.921629$ and $^{152}Sm/^{147}Sm = 1.783135$. Three analyzes of the JNDi-1 performed during the Durango TIMS session gave $^{143}Nd/^{144}Nd = 0.512106 \pm 0.000008$ (2σ). Results are presented in Table 1. They show reproducible values at the level of ±10-20 ppm for $^{143}Nd/^{144}Nd$ and $^{145}Nd/^{144}Nd$ (2σ-variation) and of ±0.5 % for $^{147}Sm/^{144}Nd$. This suggests that our Durango crystal is relatively homogeneous, isotopically and chemically, at a scale of about 10 mg. Such a conclusion cannot be extended, however, to lower scales such as those of spot sizes for which 2σ-variations reported here must be *a priori* considered as minimum heterogeneity. Measured $^{143}Nd/^{144}Nd$ and $^{145}Nd/^{144}Nd$ ratios are consistent with previous TIMS determinations (Foster and Vance, 2006; Fisher *et al.*, 2011; Yang *et al.*, 2014; Xu *et al.*, 2018), but we observe notable differences for the $^{147}Sm/^{144}Nd$ ratio with some of the data available in the literature (e.g. Yang *et al.*, 2014: their Durango crystal has a $^{147}Sm/^{144}Nd$ ratio of 0.0881), reinforcing the importance for each geochemical laboratory to characterize their Durango crystal by solution before to use it for external normalization.

Phalaborwa apatites were separated from an intrusive calcio-carbonatite sample (PhB09) coming from the Phalaborwa carbonatite Complex, South Africa. Their age is estimated to be 2060 ± 2 Ma (U-Pb isotopic age determinations on baddeleyites separated from Phalaborwa carbonatite samples similar to PhB09; Wu

et al., 2011). Phalaborwa apatites are small crystals compared to Durango, with maximum sizes in the order of 100 µm, so it was not possible to characterize a fragment of each of the crystals analyzed by LA-MC-ICPMS using TIMS. Instead, three sets of multiple apatite grains weighting between 7 and 12 mg were analyzed using the same protocol than Durango fragments D1, D2 and D3. Results are presented in Table 1. They show 2σ-variations of ±50 ppm for $^{143}Nd/^{144}Nd$ and of ±0.2 % for $^{147}Sm/^{144}Nd$. Initial $^{143}Nd/^{144}Nd$ ratios back-calculated using an age of 2060 Ma ranges between 0.509668 and 0.509674 (εNd(t2060) between -5.8 and -6.0). These are consistent values with initial ratios (εNd(t2060) between −3.4 and −7.5) determined for the Phalaborwa primary carbonatitic magma (Yuhara *et al.*, 2005; Wu *et al.*, 2011). Finally, Fogo apatites were separated from a calcio-carbonatite sample collected in a dike on Fogo Island, Cape Verde archipelago. Their age is estimated to be ~4 Ma (cf. Mata *et al.*, 2010) and TIMS analyzes performed on 50-mg of multiple grains gave $^{143}Nd/^{144}Nd$ = 0.512945 ± 0.000006 (Doucelance *et al.*, 2010).

3. Instrumentation and protocol of in-situ analysis of Nd isotopes

Neodymium isotopic measurements were performed using a Thermo Fisher Scientific™ Neptune Plus™ mass spectrometer coupled with a 193-nm wavelength Resonetics™ M-50E laser system. All analyzes were acquired at the LMV, Clermont-Ferrand, France. Prior to in-situ analyzes, apatite samples were embedded in epoxy resin blocks and polished. Cathodoluminescence (CL) images were also obtained using a Jeol JSM-5910 LM scanning electron microscope (SEM) in order to characterize internal structures of apatite grains and better decide for spot targets.

The MC-ICPMS was operated in static mode using 7 Faraday Cups. This allowed the simultaneous collection of masses 143 to 149 (Table 2). A typical run consisted of 70 cycles of measurements with an integration time of 1s, the first 15 cycles being used to evaluate the baseline level of each Faraday Cup. X skimmer cone coupled to a Jet interface sampler cone were systematically used unless reported. $^{143}Nd/^{144}Nd$ and $^{145}Nd/^{144}Nd$ isotopic ratios together with $^{147}Sm/^{144}Nd$ chemical ratios were determined in each case. Baseline and gain reductions were operated online; all other calculations were performed off-line using an in-house Microsoft Excel™ spreadsheet. Gain calibration was done at the beginning of each analytical session. Corrections for isobaric interferences, elemental and mass biases are detailed in the following subsections, whereas LA-MC-ICPMS parameters are summarized in Table 3.

3.1. Correction for isobaric interferences of Neodymium isotopes

Isotope ^{144}Nd interferes with ^{144}Sm and ^{146}Nd with $^{130}Ba^{16}O$ (barium oxide) if the analyzed material contains barium (Table 2). Barium-130 is only 0.1% of total Barium, and oxide production has been minimized at the beginning of each session of analysis ($^{146}Nd^{16}O/^{146}Nd$ ratio < 1%) meaning that the $^{132}Ba^{16}O$ signal is negligible with respect to ^{146}Nd intensity of apatite samples. For these reasons, no correction was applied to ^{146}Nd. For Sm interferences, however, we followed Yang *et al.* (2008) and Fisher *et al.* (2011) and used the 3-steps procedure described in McFarlane and McCulloch (2007) that considers an exponential law for MC-ICPMS mass fractionation (Russell *et al.*, 1978) together with the most recent determinations of Sm isotopic abundances (here illustrated for mass 144):

• *Step 1* - The measured, interference-free $^{147}Sm/^{149}Sm$ ratio is used to determine the mass bias correction factor of Sm (β_{Sm}):

$$\beta_{Sm} = \frac{ln\left[\frac{\left(^{147}Sm/^{149}Sm\right)_{true}}{\left(^{147}Sm/^{149}Sm\right)_{meas}}\right]}{ln\left[Mass\_^{147}Sm/Mass\_^{149}Sm\right]} \quad (1)$$

where subscripts *true* and *meas* denote the assumed (1.08680 - Dubois *et al.*, 1992) and measured values of the $^{147}Sm/^{149}Sm$ isotopic ratio, respectively, and $Mass\_^{147}Sm/Mass\_^{149}Sm$ is the ratio of atomic masses;

• *Step 2* - The intensity of ^{144}Sm is then calculated from that of ^{149}Sm, given the true value of $^{144}Sm/^{149}Sm$ ($^{144}Sm/^{149}Sm$ and $^{148}Sm/^{149}Sm$ ratios normalized to $^{147}Sm/^{149}Sm$ value of Dubois and co-authors are 0.22332 and 0.81407, respectively - Isnard *et al.*, 2005):

$$^{144}Sm = {}^{149}Sm \times \left(^{144}Sm/^{149}Sm\right)_{true} \times \left(Mass\_^{144}Sm/Mass\_^{149}Sm\right)^{\beta_{Sm}} \quad (2)$$

• *Step 3* - Finally, the ^{144}Sm interference is removed from the total intensity at mass 144:

$$^{144}Nd = 144_{total} - {}^{144}Sm \quad (3)$$

3.2. Correction for Neodymium mass bias

The mass bias correction factor of Nd (β_{Nd}) was deduced from the measured $^{146}Nd/^{144}Nd$ ratio, corrected for the interference of ^{144}Sm and compared to its true value (0.7219 – Wasserburg *et al.*, 1981) via the exponential law:

$$\beta_{Nd} = \frac{ln\left[\frac{\left(^{146}Nd/^{144}Nd\right)_{true}}{\left(^{146}Nd/^{144}Nd\right)_{meas}}\right]}{ln\left[Mass\_^{146}Nd/Mass\_^{144}Nd\right]} \quad (4)$$

$^{143}Nd/^{144}Nd$ and $^{145}Nd/^{144}Nd$ isotopic ratios were then calculated from their measured values corrected for ^{144}Sm:

$$^{143}Nd/^{144}Nd = \left(^{143}Nd/^{144}Nd\right)_{meas} \times \left(Mass\_^{143}Nd/Mass\_^{144}Nd\right)^{\beta_{Nd}} \quad (5)$$

$$^{145}Nd/^{144}Nd = \left(^{145}Nd/^{144}Nd\right)_{meas} \times \left(Mass\_^{145}Nd/Mass\_^{144}Nd\right)^{\beta_{Nd}} \quad (6)$$

3.3. Determination of the $^{147}Sm/^{144}Nd$ chemical ratio

Simultaneous and accurate determination of the $^{147}Sm/^{144}Nd$ chemical ratio allows recalculating initial Nd compositions of old apatites given that ages of the samples are independently known. An internal determination of $^{147}Sm/^{144}Nd$, as for Nd and Sm isotope ratios, is impossible to obtain due to the numerous effects which can potentially fractionate Sm and Nd: different vaporization rates of the two elements (Kuhn and Günther, 2003; Košler *et al.*, 2005), different element ionization rates in the plasma (Guillong and Günther, 2002), instrumental drift (Cheatham *et al.*, 1993), and also, similarly to Nd or Sm isotope ratios, mass discrimination in the MC-ICPMS (Vance and Thirlwall, 2002). Depending on the laser system and cells, sample position in laser cell can also be problematic (Fisher *et al.*, 2011). All these issues are reinforced by the fact that elemental fractionation also varies with the nature of the sample matrices (Chen *et al.*, 1999). In their paper focusing on the $^{147}Sm/^{144}Nd$ and $^{143}Nd/^{144}Nd$ in-situ analysis of monazite, Iizuka *et al.* (2011) proposed two distinct methods for acquiring the correction factor *f* between the true and measured $^{147}Sm/^{144}Nd$ ratios.

The first procedure consists to normalize unknown samples to a standard whose $^{147}Sm/^{144}Nd$ is uniform and has been independently determined (Foster and Vance, 2006). This is the way Yang *et al.* (2014) corrected their apatite Sm/Nd data, using AP2 apatite reference material as external standard. This is also the approach retained by Fisher *et al.* (2011), although they did not use a matrix-match standard but a glass enriched in light REE (LREE). The second method proposed by Iizuka *et al.* (2011) is to use an ancient monazite standard for which a $^{147}Sm/^{144}Nd$-$^{143}Nd/^{144}Nd$ isochron can be independently defined. Comparison between the standard isochron and a $^{143}Nd/^{144}Nd$ vs. measured $^{147}Sm/^{144}Nd$ plot for the same standard then allows estimating the correction factor f. Foster and Vance (2006) also proposed to correct the measured $^{147}Sm/^{144}Nd$ ratio for the instrumental mass bias using the mass bias correction factor of Nd (β_{Nd}, as defined in eq. 4). This leads to the following equation, providing that ^{144}Nd is corrected for ^{144}Sm contribution:

$$^{147}Sm/^{144}Nd = \left(^{147}Sm/^{144}Nd\right)_{meas} \times \left(Mass\_^{147}Sm/Mass\_^{144}Nd\right)^{\beta_{Nd}} \quad (7)$$

Mass bias correction factors of Nd and Sm are significantly different (McFarlane and McCulloch, 2007; Yang *et al.*, 2008) so that the choice of β_{Nd} to correct for instrumental mass bias is questioned. However, such a correction, even not accurate, allows discussing other reasons for Sm/Nd fractionation than mass bias. In the present study, we used both approaches: $^{147}Sm/^{144}Nd$ correction using eq. 7 and external calibration against the $^{147}Sm/^{144}Nd$ ratio of our Durango-apatite crystal that was measured regularly during the day-sessions of analysis of unknown apatite samples.

4. Instrumental drift at constant laser parameters

One important observation made during this study is the presence of a systematic, decreasing drift of measured $^{147}Sm/^{144}Nd$ values while keeping all instrumental parameters constant. To illustrate this key point, Figure 1 shows 48 runs of the same Durango chip standard that were all acquired with the same laser parameters (spot size = 40 µm, fluence = 3.8 J/cm^2 and frequency = 6 Hz) over five hours. $^{143}Nd/^{144}Nd$ and $^{145}Nd/^{144}Nd$ ratios are all within uncertainties of each other and show respective, 2-σ reproducibilities (2σ-variation divided by the mean value) of 178 and 157 ppm, whereas $^{147}Sm/^{144}Nd$ ratios seem to decrease continuously from ~0.0775 to ~0.0760 before to settle. The total range corresponds to a variation of ±1.2% on the average $^{147}Sm/^{144}Nd$ value (see runs #18 to 65, day-session 2, in Supplementary Table). Correcting for the drift however gives a 2-σ reproducibility of 0.7%, which is comparable to the level of heterogeneity revealed by solution analyzes of Durango fragments D1, D2 and D3.

It may be argued that such a drift is due to zoning within Durango since the analyzes are reported in the order of acquisition. Several elements argue however against a major control of zoning on the $^{147}Sm/^{144}Nd$ ratio: 1) our Durango crystal has been broken independently of the c-axis, along which zoning can be potentially observed; 2) the spots reported on Figure 1 are all located in a limited area of our Durango crystal: they form a cluster but do not draw a traverse; and 3) cathodoluminescence imaging of our Durango grain did not show any concentric zoning (see Supplementary Fig. S1). Finally, the analysis at constant MC-ICPMS and laser parameters of an homogeneous, Sm-doped JNDi glass in order to avoid the possible contribution of an heterogeneity of our natural standard show similar results (Figs 2A,B,C). $^{143}Nd/^{144}Nd$ and $^{145}Nd/^{144}Nd$ ratios have reproducible values within uncertainties, whereas $^{147}Sm/^{144}Nd$ decrease before to settle. The drift induced a variation up to ±0.8% over five hours which has to be considered when trying to

evaluate the most accurately possible the $^{147}Sm/^{144}Nd$ ratio of the analyzed material. Such variations are correlated to the average ^{146}Nd ion beam signal (Fig. 2D) suggesting that the decreasing drift is a response to the decreasing ^{146}Nd signal that is generally observed when we keep instrumental parameters constant.

5. Influence of laser parameters on the determination of $^{143}Nd/^{144}Nd$, $^{145}Nd/^{144}Nd$ and $^{147}Sm/^{144}Nd$ ratios

All the data presented in this section have been acquired during seven day-sessions over a period of one year. In the following, we discuss the possible influence of the laser parameters (the size of the spot, the fluence and the frequency of the laser range from 33 to 93 µm, from 3.4 to 4.6 J/cm^2, and from 5 to 8 Hz, respectively) together with that of He/N_2 gas flows on Nd isotopic compositions and $^{147}Sm/^{144}Nd$ ratios. Attention is focused more specifically on 40-µm laser spots since this corresponds to a reasonable size for apatite crystals in most geological samples.

5.1. Laser spot size

Figure 3 shows $^{143}Nd/^{144}Nd$ and $^{145}Nd/^{144}Nd$ isotope ratios together with $^{147}Sm/^{144}Nd$ chemical ones obtained for Durango apatite during day-session 1. The data are reported in chronological order of acquisition. Measurements reported with a red square have been performed with constant frequency and fluence (6 Hz, 3.8 J/cm^2) but various sizes of spot (93, 40 and 33 µm). The three sets of data show reproducible values for $^{143}Nd/^{144}Nd$ and $^{145}Nd/^{144}Nd$ isotope ratios at the level of 79-85 ppm for 93-µm-spot measurements (79 ppm for $^{143}Nd/^{144}Nd$ and 85 ppm for $^{145}Nd/^{144}Nd$), and 132-187 ppm and 158-247 ppm, for 40- and 33-µm spot sizes (Figs. 3A,B and Supplementary Table). These reprodubilities are not as precise as those obtained by TIMS for the three Durango fragments but all analysis performed at different spot sizes give $^{143}Nd/^{144}Nd$ and $^{145}Nd/^{144}Nd$ within uncertainties. This suggests that the weaker reproducibility of in-situ measurements results mainly from the small ion beam signals and consequently the size of the laser spot has no influence on the isotopic composition of the apatite sample.

On the other end, average $^{147}Sm/^{144}Nd$ ratios vary significantly, increasing from 0.0744 to 0.0784 when the spot size is decreasing from 93 to 40 µm (Fig. 3C). Such a variation of about ±3% on the average $^{147}Sm/^{144}Nd$ value (that was also observed to a lesser extent during day-session 3, with $^{147}Sm/^{144}Nd$ ratios equal to 0.0751-0.0755 and 0.0773-0.0777 for spot sizes of 93 and 40 µm, respectively; see Supplementary Table) is much greater than that resulting from the chemical heterogeneity of the Durango crystal. Comparison with analyzes operated at constant parameters (section 4, Figure 1) shows that the variation of the spot size is likely to be responsible for at least 2/3 of the variation of the $^{147}Sm/^{144}Nd$ ratio during day-session 1. This confirms previous results by Fisher *et al.* (2020) that showed that the spot size controls how Sm isotopes are sampled relative to Nd ones during ablation. Variations they reported for the $^{147}Sm/^{144}Nd$ ratio when changing the spot size between 120 and 40 µm are in the order of 5%.

5.2. Fluence of the laser

At constant spot-size and frequency, the fluence controls the amount of ablated material, and therefore the sampling of apatite crystals. In Figures 3A,B, $^{143}Nd/^{144}Nd$ and $^{145}Nd/^{144}Nd$ isotopic ratios measured at 6 Hz with a spot size of 40 µm and a laser fluence varying from 3.4 to 4.6 J/cm^2 (around 0.5 J/cm^2 step;

red symbols) are identical within error-bars. The $^{147}Sm/^{144}Nd$ chemical ratio varies slightly between these different conditions but average values recorded during the session (large symbols) are also all within uncertainties (Fig. 3C). Analyzes performed during day-session 2 with the same conditions (40 µm - 6 Hz - 3.4 to 4.6 J/cm^2) show similar results. The $^{143}Nd/^{144}Nd$ and $^{145}Nd/^{144}Nd$ ratios display the same values within error-bars, whereas $^{147}Sm/^{144}Nd$ variations are observed but cannot be correlated with the intensity of the fluence (Fig. 4). All the results strongly suggest that the fluence range used here has no effect on the measurements of isotopic and chemical compositions of the apatites. The variations of the chemical ratio are of 1% during day-session 1 and of 2.5% during day-session 2 (2-σ variations considering individual runs that scatter slightly more than average values). As seen before, up to 1% of theses variations can be attributed to the instrumental drift observed during a day-session. The remaining scatter is most probably related to the slight chemical heterogeneity of the Durango chip.

5.3. Frequency of the laser

Similarly to the fluence, the frequency of the laser influences the amount of ablated material and thus can induce fractionation of Sm and Nd during ablation. Analyzes performed with 40-µm spots and 3.8-J/cm^2 fluence (reported with yellow- and red squares in Figure 3) show that a change from 6 to 8 Hz does not modify the Nd isotopic ratios significantly but results in a decrease of error-bars. This is also the case when considering 33-µm-spots and 6- to 7-Hz variations (blue- and red diamonds in Figure 3). Conversely, the associated, average $^{147}Sm/^{144}Nd$ ratios seem to vary with the frequency. However, in the first case, we observe an increase of the chemical ratio with decreasing frequency (8 to 6 Hz), and a decrease of the chemical ratio in the second case (7 to 6 Hz). In both cases, the $^{147}Sm/^{144}Nd$ individual measurements that compose average values are quite dispersed. However, the internal dispersion is of the same magnitude as the difference between the frequency sets for a given spot-size. Thus, with our current dataset, no relationship is observable between$^{147}Sm/^{144}Nd$ values and laser frequencies.

5.4. He and N_2 gas flows

Gas flows arriving at the cell (He, N_2) can be punctually modified during a day-session of analysis when changing a sample block or when optimizing the signal while keeping the oxides to a low level (Nd^+O/Nd^+ < 1%). Furthermore, it cannot be excluded that the He gas tank also arrives to exhaustion, thus forcing to change it during a day-session. Such flow modifications are not of the same magnitude. A sample exchange will lead to nitrogen shut-down and helium flow diminution (down to ~100 ml/min) before all flows are set back to their initial values, whereas He and N_2 flows to optimize the signal and minimize oxides will be modified in a lesser extent (addition or removal < 150 ml/mn for He and ~1 ml/mn for N_2). In this contribution, we tune both gas flows and the z-torch position to control oxide formation. During the course of the study, we experienced all these gas flow changes and we observed that they have had a great impact on the $^{147}Sm/^{144}Nd$ ratios.

The helium tank was changed during day-session 2 after 17 Durango measurements (Fig. 4) and therefore N_2 and He were set to 0 for several minutes. The change had no consequence on isotope results. $^{143}Nd/^{144}Nd$ and $^{145}Nd/^{144}Nd$ ratios show identical values before and after helium-tank exhaustion. On the contrary, $^{147}Sm/^{144}Nd$ chemical ratios varied significantly: they slightly increased after the He tank change

and then stabilized (Fig. 4C). This observation strongly suggests that $^{147}Sm/^{144}Nd$ ratios are sensitive to extremely fine gas flow variations since N_2 and He flows were set back to initial values after tank change.

Such a conclusion is also supported by measurements performed on a Sm-doped JNDi glass during day-sessions 6 and 7, during which we proceeded to a sample exchange. In both cases, while $^{143}Nd/^{144}Nd$ and $^{145}Nd/^{144}Nd$ ratios show constant values within error-bars, $^{147}Sm/^{144}Nd$ systematically jump to higher values after the sample exchange (see the last run but one of day-session 6 for 53-µm measurements and the last one of day-session 7, Figure 2C). The variation of the $^{147}Sm/^{144}Nd$ ratio reached 1.9% during day-session 7. The sample exchange consisted here in lowering He to 100 ml/mn and N_2 to 0, changing the sample, which takes several minutes, and setting the He and N_2 flows up to their initial values once the new mounts were in. The results acquired during day-session 6 thus show that within the 10 mn following the sample exchange, the $^{147}Sm/^{144}Nd$ ratio measurements are affected before to settle back to the trend of the instrumental drift.

The previous observations were made while bringing back the gas flows back to their initial values. During several sessions, we also attempted to change the He flow values to lower oxides. Figure 5 show measurements that were operated alternatively in the same Durango grain and in a NIST SRM 610 glass sample before and after He flow adjustment operated in order to decrease the oxide level from 3% down to 0.4%. Correction factors determined for $^{143}Nd/^{144}Nd$ and $^{145}Nd/^{144}Nd$ ratios show identical values within error-bars for both samples, and also before and after the He flow modification, whereas correction factors for $^{147}Sm/^{144}Nd$ show significant variations up to 1%. Interestingly, $^{147}Sm/^{144}Nd$ correction factors move in opposite ways: values decrease for Durango, while they increase for NIST SRM 610.

6. Influence of laser parameters on the within-run variation of the $^{147}Sm/^{144}Nd$ chemical ratio

Once the corrections described in section 3 have been performed, the $^{143}Nd/^{144}Nd$ and $^{145}Nd/^{144}Nd$ isotopic ratios measured for the n cycles of a single spot analysis show constant values inferring that the corrections are robust. Conversely, variable values of the $^{147}Sm/^{144}Nd$ chemical ratio due to laser induced elemental fractionation or down-hole fractionation that occurs when measuring inter-element ratios (Iizuka *et al.*, 2011; Fisher *et al.*, 2017; 2020) are expected. Correction for Sm/Nd fractionation indeed only considers Nd-isotope mass-discrimination that proceeds mainly in the interface region.

Figure 6 compiles cycle-to-cycle $^{147}Sm/^{144}Nd$ ratios that were measured in our Durango apatite grains for different laser parameters. Various evolutions can be observed within a single analysis: uniform increase, «V-shape» or «inverse V-shape» patterns. Such cycle-to-cycle variations are very reproducible as illustrated on Figure 7. This figure reports the $^{147}Sm/^{144}Nd$ patterns observed in ten consecutive analyzes for three distinct sets of laser parameter values. Relationships between laser parameters and cycle-to-cycle evolutions, however, remain unclear. Decrease of the spot-size for constant fluence and frequency values has impact on $^{147}Sm/^{144}Nd$ behavior from «inverse V-shape» to uniform increase (Fig. 6C to Fig. 6B to Fig. 6D). Decrease of the fluence (for constant spot-size and laser frequency) leads to «inverse V-shape» $^{147}Sm/^{144}Nd$ evolutions (Fig. 6B to Fig. 6A), whereas increase of the same parameter conducts to « V-shape» patterns (Fig. 6B to Fig. 6E). Lastly, increase of the laser frequency is able to change the $^{147}Sm/^{144}Nd$ pattern from monotonous increase to «V-shape» (Fig. 6B to Fig. 6G), although it can also have no significant effect (Fig. 5F to Fig. 5H). When analyzing other apatite crystals than Durango with the same laser parameters (namely Fogo Island, Cape Verde, and Phalaborwa, South Africa), different within-run variations of $^{147}Sm/^{144}Nd$ ratios

are observed. Figures 6J and 6K compare cycle-to-cycle results obtained in apatite grains from the two carbonatites that have been cross-measured with Durango chips. For identical laser parameters, Fogo and Phalaborwa apatite grains show clearly distinct patterns. Fisher *et al.* (2020) reported within-run $^{147}Sm/^{144}Nd$ evolutions measured in the Tory Hill apatite for spot sizes varying from 50 to 130 µm. All patterns show an uniform increase, except for the smallest spot size for which they are flat. They also noticed that spot sizes of 50 µm produce accurate $^{147}Sm/^{144}Nd$ ratios (in comparison to their TIMS value), whereas largest ones give lower, erroneous values. Such a relationship is not so clear for our Durango data. All measurements reported in Figure 6 and related to 40 and 33 µm spot sizes have average $^{147}Sm/^{144}Nd$ ratios between 0.0775 and 0.0785, which is higher than the TIMS value. On the contrary, 93- and 53-µm analyzes have average $^{147}Sm/^{144}Nd$ values slightly lower than our TIMS determination. All these observations show that the observed patterns depend on the laser parameters but also on the composition of the apatite. However, even if these patterns have been identified, we will see in the next section that their average value are reproducible within ~1% or better (see also Supplementary Table).

7. Reproducibility and accuracy of apatite analysis on different Durango chips

Figure 8 compiles $^{143}Nd/^{144}Nd$ and $^{145}Nd/^{144}Nd$ isotopic ratios together with $^{147}Sm/^{144}Nd$ chemical ratios measured in the same Durango grain (chip #1) during 3 day-sessions of acquisition (3 sessions over one month: 2 successive days and another one 30 days later, for which 85, 77 and 59 runs have been acquired; the data are reported in chronological order of acquisition). $^{143}Nd/^{144}Nd$ and $^{145}Nd/^{144}Nd$ ratios show comparable reproducibility with 2sd-values comprised between 139 and 179 ppm and between 111 and 170 ppm, respectively (Figs. 8A,B). While clear differences of mean $^{143}Nd/^{144}Nd$ ratios between sessions can be observed (up to 174 ppm), mean $^{145}Nd/^{144}Nd$ are one order of magnitude lower (17 ppm). However, these variations between mean values are all within uncertainties of each other. Finally, except for day-session one, the $^{143}Nd/^{144}Nd$ ratios mean values are within error of the Durango-chip TIMS values. It should be mentioned that individual $^{143}Nd/^{144}Nd$ are lower than TIMS values for most of the runs, while $^{145}Nd/^{144}Nd$ scatter around the TIMS determination. Mean $^{147}Sm/^{144}Nd$ values are reproducible at the level of 0.8% (Fig. 8C). However, the reproducibility within sessions is far lower and the $^{147}Sm/^{144}Nd$ variations are such that error-bars associated to mean values for each session are all overlapping with each other over the 3 days of acquisition. Considering these important uncertainties, they are also in agreement with TIMS values although calculated mean values are all higher than TIMS values. Such observation is likely to be a coincidence since: (i) individual $^{147}Sm/^{144}Nd$ ratios do not scatter around calculated mean values but show different evolutions depending of the day considered; and (ii) $^{147}Sm/^{144}Nd$ ratios reported in Figure 8C are not corrected for Sm/Nd elemental bias.

Measurements made on two other Durango chips (chips #2 and #3; spot size = 40 µm; fluence comprised between 4.5 and 4.8 J/cm^2; and frequency between 6 and 10 Hz) during the third day-session confirm all the above observations (Fig. 9). Most of the $^{143}Nd/^{144}Nd$ ratios have a value lower than that determined by TIMS. On the contrary, $^{145}Nd/^{144}Nd$ determinations scatter around the TIMS value, whereas $^{147}Sm/^{144}Nd$ ones are significantly distinct from one Durango chip to another and also within a single chip. These measurements confirm that our Durango crystal is homogeneous for Nd isotopes: $^{143}Nd/^{144}Nd$ and $^{145}Nd/^{144}Nd$ ratios define similar ranges of variations of 150 and 120 ppm for the 3 chips. The variation of the chemical ratio is of 1.5% (2-σ variations considering all the individual runs) and it is likely to be controlled by the

heterogeneity of our Durango crystal, although small variations of measurements conditions explaining part of the $^{147}Sm/^{144}Nd$ jumps cannot be excluded. The difference in accuracy between $^{143}Nd/^{144}Nd$ and $^{145}Nd/^{144}Nd$ ratios does not result from an inaccurate TIMS value of the Durango apatite. Indeed, similar systematics are observed for the measurements made on apatite grains from Fogo (Cape Verde Islands) and Phalaborwa (South Africa; Fig. 10).

Systematic offsets between $^{143}Nd/^{144}Nd$ ratios measured by LA-MC-ICPMS and their corresponding TIMS value have been previously reported (e.g. Newman *et al.*, 2009; Newman, 2012; Xu *et al.*, 2015; Fisher *et al.*, 2011; Spandler *et al.*, 2016). Fisher *et al.* (2020) have recently suggested that the accuracy of $^{143}Nd/^{144}Nd$, $^{145}Nd/^{144}Nd$ and $^{147}Sm/^{144}Nd$ measurements can be greatly influenced by the total sample gas flow and therefore the production of oxides. Here we explore if the difference of offset values (especially for the $^{143}Nd/^{144}Nd$ ratio) observed between day-sessions 1 to 3 (Fig. 8A) could be related to our sample gas flow. Our measurements were all performed with a flow in the range 0.974 to 0.984 l/mn. This approximatively corresponds to the threshold value from which inaccuracy of measured ratios is observed by Fisher *et al.* (2020; about 0.95 l/mn). Our sample gas flow may then explain why lower-than-TIMS $^{143}Nd/^{144}Nd$ ratios were systematically measured together with variable values from a day-session to another one. However, following Fisher *et al.* (2020), this would have implied inaccurate $^{145}Nd/^{144}Nd$ ratios which is not observed (Fig. 8B). Thus, the deviations described by Fisher *et al.* (2020) related to the sample gas flow are most certainly comprised in the error-bars of our measurements, but they do not explain our observations. The difference of offset values between day-sessions 1 to 3 is certainly related to a slight change in the instrument behavior.

Inaccurate $^{143}Nd/^{144}Nd$ ratios relative to $^{145}Nd/^{144}Nd$ may be also related to an inappropriate correction for mass discrimination. In this paper, we consider that the mass-discrimination factor β^{Nd} is the same for the three $^{146}Nd/^{144}Nd$, $^{143}Nd/^{144}Nd$ and $^{145}Nd/^{144}Nd$ ratios (eq. 4). On the other hand, Thirlwall (2002) proposed that β^{Nd} may be a function of the considered isotopic ratio, so that $\beta_{143/144} < \beta_{145/144} < \beta_{146/144}$. In this case, determining the β^{Nd} factor with the $^{146}Nd/^{144}Nd$ ratio may result in an over-correction of the $^{143}Nd/^{144}Nd$ and $^{145}Nd/^{144}Nd$ ratios, with the bias being more important for $^{143}Nd/^{144}Nd$. For instance, Vance and Thirlwall (2002) when normalizing MC-ICPMS solution data to $^{146}Nd/^{144}Nd$ ratio, observed inaccurate $^{143}Nd/^{144}Nd$ and $^{145}Nd/^{144}Nd$ ratios by 100 and 30 ppm, respectively. Such a factor of ~3 in the bias between $^{143}Nd/^{144}Nd$ and $^{145}Nd/^{144}Nd$ is not observable in our data. Furthermore, if the $^{143}Nd/^{144}Nd$ bias was related to an inappropriate mass-discrimination law such as proposed by Vance and Thirlwall (2002), we should expect to observe a relationship between the $\Delta^{143}Nd/^{144}Nd$ (where $\Delta^{143}Nd/^{144}Nd$ is the difference between the observed $^{143}Nd/^{144}Nd$ ratio and its true, TIMS determined value) and the β^{Nd} factor determined with $^{146}Nd/^{144}Nd$, which is not the case (Supplementary Fig. S2).

As an alternative hypothesis, we also explored the effect of the ^{144}Sm correction on ^{144}Nd by considering distinct sets of values for the $^{147}Sm/^{149}Sm$ and $^{144}Sm/^{149}Sm$ ratios (section 3.1). Using $^{144}Sm/^{149}Sm = 1.08504$ and $^{147}Sm/^{149}Sm = 0.22245$ (Brandon *et al.*, 2009; Rankenburg *et al.*, 2006) has no influence on the Nd isotopic ratios. Using recent values published by Bouvier and Boyet (2016), i.e., $^{144}Sm/^{149}Sm = 1.08506$ and $^{147}Sm/^{149}Sm = 0.22336$, increases the $^{143}Nd/^{144}Nd$ and $^{145}Nd/^{144}Nd$ ratios by 100 and 30 ppm, respectively. The $^{143}Nd/^{144}Nd$ value, however, remains too low (see Supplementary Fig. S3). Interestingly, the effect of the Sm correction documented here is of the same order of magnitude than biases observed by Vance and Thirlwall (2002) and attributed to the use of an inappropriate mass-discrimination law.

Finally, we investigated the effect of the sampling system. Indeed, previous workers have tested the influence of sample- and skimmer-cone combination on Nd isotope measurements (e.g. Newman *et al.*, 2009; Newman, 2012; Xu *et al.*, 2015). In particular, Newman (2012) indicated that the association of Jet-cone and X-skimmer allows to greatly improve the analytical sensitivity compare to the N-cone/H-Skimmer association. However, they also indicate that the X-skimmer introduces additional contributions to the instrumental mass fractionation that cannot be corrected for by using a classical exponential correction. These studies clearly show that the use of X-skimmer induces the formation of Nd^+O which alters the accuracy of the measurements. Finally, results of these previous studies show that by minimizing the Nd^+O/Nd^+ (<1%), measured isotope ratios tend to approach the "true" value. Measurements done on our Durango chip with H-skimmer coupled to sampler cone (see Supplementary Fig. S4 and Supplementary Table) have $^{143}Nd/^{144}Nd$ and $^{145}Nd/^{144}Nd$ ratios scattering around the TIMS values (although average $^{143}Nd/^{144}Nd$ values remain slightly lower than those determined by TIMS) so that both isotope ratios are now accurate. Within-run error-bars reported on isotopic ratios, however, are higher by a factor 2 to 3 than those determined with the reference protocol (X-skimmer and Jet-cone) for the same laser parameters and the 2-σ reproducibility of $^{143}Nd/^{144}Nd$ is degraded to 400 ppm (4 εNd-units). Considering the $^{147}Sm/^{144}Nd$ chemical ratio, all measured values are higher than the TIMS determination, in agreement with some of our "reference" measurements.

All of the above assumptions (high sample gas flow, inaccurate mass discrimination law, inappropriate Sm isotopic composition, influence of the sampling system) are not mutually exclusive. On the contrary, they surely all participate, to a certain extent, to the variations observed from spot to spot, or to the inaccuracy of some corrected ratios. Small variations in the setting of the instrumentation, from a day-session to another one, may also play a role. In any case, none of the tests realized during this study allows both accurate and precise isotope and chemical ratios. Therefore, the measured data must necessarily be normalized against an external, known reference.

8. External normalization against Durango apatite

All the recent studies on in-situ determination of $^{147}Sm/^{144}Nd$ in apatite have concluded that an external normalization of measured ratios is mandatory and that a matrix-matched standard is required (Fisher *et al.*, 2020; and references therein). Our intercalated NIST610/Durango data agree perfectly with this prerequisite (Fig. 5). Although both samples were measured using the same analytical conditions, $^{147}Sm/^{144}Nd$ correction factors determined for NIST SRM 610 and Durango are significantly different.

Figure 11 presents normalized Durango ratios (data acquired during day-session 2 at constant laser parameters: spot size = 40 µm, fluence = 3.8 J/cm^2, and frequency = 6 Hz) that are obtained when considering that one measurement every two is an unknow, and compares them with raw values (corrected for baseline, gain, Sm interference and mass discrimination). Recalculated $^{143}Nd/^{144}Nd$, $^{145}Nd/^{144}Nd$ and $^{147}Sm/^{144}Nd$ ratios all scatter around their respective TIMS determination and show total reproducibilities of 235 ppm, 230 ppm and 1.36% (n = 46), respectively. These values are up to five times higher than those obtained by Fisher *et al.* (2011) and Yang *et al.* (2014) for $^{143}Nd/^{144}Nd$ and $^{145}Nd/^{144}Nd$ ratios (94 and 55 ppm, and 90 and 83 ppm, respectively), but surprisingly they are far better for $^{147}Sm/^{144}Nd$. Such differences have to be considered, however, with care. Fisher *et al.* (2011) made their analyzes with a laser spot size of 148 µm and normalized data to a LREE glass, whereas measurements by Yang and collaborators (2014) were

performed with a laser spot size of 90 µm and normalized to AP2 apatite. In our study we considered smaller spot sizes of 40 µm that seemed to us more reasonable if we want to resolve zoning variations in apatite crystals in geological samples. Also, it has to be mentioned that the 90-ppm reproducibility published by Yang *et al.* (2014) for $^{143}Nd/^{144}Nd$ corresponds to the two-standard-deviation of 8 sessions during which the reproducibility was up to 120 ppm. As a better comparison, our 93-µm analyzes give similar reproducibilities of 80 and 85 ppm for $^{143}Nd/^{144}Nd$ and $^{145}Nd/^{144}Nd$.

Fogo and Phalaborwa apatite measurements were also normalized to the Durango standard. In the case of Fogo, apatites were separated from a 'zero'-age carbonatite sample and therefore normalized Nd ratios are expected to fit with TIMS determinations that were performed on both apatite and whole carbonatite samples (Doucelance *et al.*, 2010). For Paleoproterozoic Phalaborwa apatites, however, comparison between normalized data and TIMS values may be less pertinent. It can be reasonably assumed that the initial $^{143}Nd/^{144}Nd$ ratios of apatites were all identical but we cannot exclude small variations of their initial $^{147}Sm/^{144}Nd$, so that radioactive decay of ^{147}Sm to ^{143}Nd over 2060 Ma may have led to actual Nd compositions and $^{147}Sm/^{144}Nd$ ratios varying from one crystal to another. Since the TIMS measurements were performed on crystals distinct from those analyzed in-situ, some discrepancies may thus appear between the two determinations. This tends to agree with the poorer reproducibility of PhB09 $^{143}Nd/^{144}Nd$ and $^{147}Sm/^{144}Nd$ TIMS measurements (Table 1) and also with the large range of variations of the ^{146}Nd ion beam signal that was recorded in Phalaborwa apatite grains (Supplementary Table). A better way to interpret these values consists then in comparing initial $^{143}Nd/^{144}Nd$ ratios recalculating from both TIMS values and Durango-normalized, in-situ data. Results for Fogo and Phalaborwa apatites are reported in Figure 12. Normalization to Durango standard allows to retrieve accurate, measured (Fogo) and age-corrected (Phalaborwa), $^{143}Nd/^{144}Nd$ ratios relative to the TIMS values. Associated reproducibilities are better than those reported for Durango apatite for 40-µm spot sizes with 123 ppm (1.2 εNd-units) for Phalaborwa initial Nd ratio and between 82 and 144 ppm (0.8 and 1.4 εNd-units) for Fogo $^{143}Nd/^{144}Nd$ ratio, respectively. Such a gain in reproducibility most likely relates to the higher Nd contents of Fogo and Phalaborwa apatite grains relative to Durango (~2000 ppm against ~1000 ppm, see Table 1 and Doucelance *et al.*, 2010). We are aware that Fogo and Phalaborwa apatites represent a limited set of samples, but these two last comparisons strongly suggest that our Durango crystal can be used as an external standard for recent and ancient (2 Ga) samples. This conclusion is another argument to confirm that the slight Sm/Nd heterogeneity of our standard is limited to maximum ±1-1.5%. Fisher *et al.* (2020) have indeed shown that significant εNd deviations (> 1 εNd-unit) from the true value are related to overestimate of at least 2% of the $^{147}Sm/^{144}Nd$ ratio for an age of 2 Ga.

9. Application to natural apatites

In this contribution, we focused our analyzes in apatite crystals extremely rich in LREE (several thousands of ppm of Nd) such as commonly referred in carbonatite complexes (e.g. Djeddi, 2019). Here, we show that the Sm-Nd in-situ technique applied to apatites is particularly powerful for carbonatite samples even at a small spot size, thus allowing the analysis of the finer zoning when this is required. However, the size of the spot needed for such analysis is greatly depending on the igneous apatite content and therefore on the magma from which it grew up. Recent, Sm-Nd in-situ papers (e.g. Hammerli *et al.*, 2019; Fisher *et al.*, 2020) focused on apatite grains from Archean TTG samples that have low REE contents compared to that of Durango and therefore necessitate a much bigger spot than the 40-µm spot size used in this study.

In such material, precise Sm-Nd measurements are challenging. Sm/Nd-zoned regions have resulted in contrasted Nd isotope compositions with time (Fisher *et al.*, 2017) and different zones are more likely to be mixed in a single big spot. On the other hand, apatites from other magmas occurring through geological times such as sanukitoids or typical Basalt Andesite Diorite Rhyolite suite (BADR) can have LREE contents comparable to that of Durango (Bruand *et al.*, 2020). They are also good candidates for Sm-Nd in-situ analysis.

From a general point of view, measurements done with a spot-size of 40 microns in apatite with a Nd content lower than Durango will certainly result in important error-bars on both isotopic and chemical ratios thus limiting their interpretations. In this case, programmed-raster analyzes on cathodoluminescence-imaged apatite crystals allow to increase the counting statistics and thus decrease within-run errors. Figure 13 compares raster (length ~150 µm) and spot measurements operated one after the other during day-session 2 with the following laser parameters (40 µm - 3.8 J/cm^2 - 6 Hz). $^{143}Nd/^{144}Nd$, $^{145}Nd/^{144}Nd$ and $^{147}Sm/^{144}Nd$ ratios show fully consistent values between the two sets of data (the $^{147}Sm/^{144}Nd$ variation between the two raster runs is included in the Sm/Nd heterogeneity of Durango). More importantly, within-run error-bars are divided by a factor 2-3 for each ratio (see also Supplementary Table, day-session 2).

10. Summary

In this contribution, we show as previously done (Fisher *et al.*, 2011; Spandler *et al.*, 2016) that results obtained using Jet-interface and X-skimmer reveal a systematic shift between $^{143}Nd/^{144}Nd$ ratios corrected for Sm contribution and for mass discrimination and their true values, while $^{145}Nd/^{144}Nd$ values agree well. We also show that the spot size, the fluence and the frequency of the laser have no influence on the accuracy of Nd ratios. At most, the values used for these parameters can lead to better signals, and therefore more precise data. We confirm as previously proposed (Newman, 2012; Xu *et al.*, 2015) that accurate Nd ratios can be obtained by using N-cone and H-Skimmer which results in a much lower precision.

In this study, we focused our attention on testing the laser parameters and their influence on the $^{147}Sm/^{144}Nd$ ratio during LA-MC-ICPMS measurements on Durango apatite and both NIST SRM 610 and Sm-doped JNDi synthetic glasses when it was necessary. We confirm the recent observation that the $^{147}Sm/^{144}Nd$ ratio correlates negatively with the spot size (Fisher *et al.*, 2020), but more importantly we show the different contributions that the other laser parameters or a simple sample exchange can have on this ratio. Our main conclusions reveal that the fluence and the frequency of the laser in the range of values that were tested have no influence on the measurement of the $^{147}Sm/^{144}Nd$ ratio. However, we identified that our instrument presents a systematic decreasing drift with time that can account for up to 50% of the variation observed on Durango. This drift, if there is no change in the analysis conditions, settles half-way through five hours of a day-session before to define a plateau. Measured $^{147}Sm/^{144}Nd$ ratios can be also affected by very punctual gas flow changes induced for example by a sample exchange. In this case, it is wise to monitor the $^{147}Sm/^{144}Nd$ values on standards in the 10 minutes following the sample exchange and wait for the stabilization of the chemical ratio. More generally, the chemical ratio is extremely sensitive to the settings made during the analysis session (oxide minimization, z optimization, ...). Thus, settings have to be chosen at the beginning of the session and maintained constant all along.

Considering all these results, we favor the use of higher sensitivity sampling system (Jet-interface and X-skimmer) with a control on the Nd^+O/Nd^+ production (<1%) and the use of a matrix-matched, well-

characterized standard measured with the same laser and MC-ICPMS parameters than samples as external normalization. Our Durango crystal is homogeneous for Nd isotopic ratios, and slightly heterogeneous for Sm/Nd at the level of ±1-1.5%. Using it as reference material we retrieve accurate $^{143}Nd/^{144}Nd$ ratios for recent (Fogo) and 2060-Ma-old (Phalaborwa) carbonatitic apatites. Precisions determined for a laser spot of 40 µm (reasonable size for apatite crystals in most geological samples) are in the order of 125-150 ppm (1.3-1.5 εNd-units) for $^{143}Nd/^{144}Nd$. Such values allow to discuss the source origin of altered samples, whatever their age, that would not be possible to document as a whole. Although Durango normalization is appropriate for the Paleoproterozoic carbonatitic material studied in this contribution, the slight heterogeneity of this natural apatite may also be a limit in back-calculating accurate initial Nd ratios of older samples. Carbonatite apatites have moreover extremely high Nd contents of several thousands of ppm allowing good precision with a 40-µm spot size. Such a spot size may be a limit, however, to resolve zoning in some igneous apatites such as the ones that are more depleted in LREE (e.g. Archean TTG, Bruand *et al.*, 2020). Raster analyzes for a spot size of 40 µm and a length of 150 µm in imaged apatite crystals are able to improve the precision of the measurements by a factor 2-3. This would be a good alternative to improve the precision of less concentrated igneous apatites.

Acknowledgments

The authors would like to thank Tahar Hammouda for the Durango apatite chip (initially provided by the Smithsonian National Museum of Natural History) and for stimulating discussions during the course of measurements. Constructive reviews by Christopher Fisher and Tsuyoshi Iisuka were also greatly appreciated and helped to greatly improve the manuscript. This work has received funding from the ClerVolc Labex and from the Auvergne Region (E.B. fellowship). This is Laboratory of Excellence ClerVolc contribution number XXX.

References

- Bouvier A., Boyet M. (2016) Primitive Solar System materials and the Earth share common initial ^{142}Nd abundance. *Nature* 537, 399-402.
- Brandon A.D., Lapen T.J., Debaille V., Beard B.L., Rankenburg K., Neal C. (2009) Re-evaluating 142Nd/144Nd in lunar mare basalts with implications for the early evolution and bulk Sm/Nd of the Moon. *Geochim. Cosmochim. Acta* 73, 6421-6445.
- Bruand E., Storey C., Fowler M. (2014) Accessory phases (titanite, apatite, zircon) behaviour in late Caledonian high Ba-Sr plutons, Scotland: petrogenetic and source implications. *J. Petrol.* 55, 1619-1651.
- Bruand E., Fowler M., Storey C., Laurent O., Antoine C., Guitreau M., Heilimo E., Nebel O. (2020) Accessory mineral constraints on crustal evolution: elemental fingerprints for magma discrimination. *Geochem. Persp. Let.* 13, 7-12.
- Carlson R.W., Lugmair G.W. (1979) Sm-Nd constraints on early lunar differentiation and the evolution of KREEP. *Earth Planet. Sci. Lett.* 45, 123-132.
- Cheatham M.N., Sangrey W.F., White W.M. (1993.) Sources of error in external calibration ICP-MS analysis of geological samples and an improved non-linear drift correction procedure. *Spectroc. Acta B* 48, 487-526.

- Chen Z. (1999) Inter-elemental fractionation and correction in laser ablation inductively coupled plasma mass spectrometry. *J. Anal. At. Spectrom.* 14, 1823-1828.
- Djeddi A. (2019) Petrogenesis of Proterozoic carbonatites and alkaline magmas from Ihouhaouene: In Ouzzal terrane, Western Hoggar, Algeria. *PhD thesis*, https://hal.archives-ouvertes.fr/tel-02379077.
- Doucelance R., Hammouda T., Moreira M., Martins J.C. (2010) Geochemical constraints on depth of origin of oceanic carbonatites: The Cape Verde case. *Geochim. Cosmochim. Acta* 74, 7261-7282.
- Dubois J.C., Retali G., Cesario J. (1992) Isotopic analysis of rare earth elements by total vaporization of samples in thermal ionization mass spectrometry. *Int. J. Mass Spectrom. Ion Processes* 120, 163-177.
- Fisher C.M., McFarlane C.R.M., Hanchar J.M., Schmitz M.D., Sylvester P.J., Lam R., Longerich H.P. (2011) Sm–Nd isotope systematics by laser ablation – multicollector - inductively coupled plasma mass spectrometry: Methods and potential natural and synthetic reference materials. *Chem. Geol.* 284, 1-20.
- Fisher C.M., Bauer A.M., Luo Y., Sarkar C., Hanchar J.M., Vervoort J.D., Tapster S.R., Horstwood M., Pearson D.G. (2020) Laser ablation split-stream analysis of the Sm-Nd and U-Pb isotope compositions of monazite, titanite, and apatite – Improvements, potential reference materials, and application to the Archean Saglek Block gneisses. *Chem. Geol.* 539, 119493.
- Flowers R.M., Ketcham R.A., Shuster D.L., Farley K.A. (2009) Apatite (U–Th)/He thermochronometry using a radiation damage accumulation and annealing model. *Geochim. Cosmochim. Acta* 73, 2347-2365.
- Foster G.L., Vance D. (2006) In situ Nd isotopic analysis of geological materials by laser ablation MC-ICP-MS. *J. Anal. At. Spectrom.* 21, 288-296.
- Garçon M., Boyet M., Carlson R.W., Horan M.F., Auclair D., Mock T.D. (2018) Factors influencing the precision and accuracy of Nd isotope measurementsby thermal ionization mass spectrometry. *Chem. Geol.* 476, 493-514.
- Guillong M., Günther D. (2002) Effect of particle size distribution on ICP-induced element fractionation in laser ablation-inductively coupled plasma-mass spectrometry. *J. Anal. At. Spectrom.* 17, 831-837.
- Hammerli J., Kemp A.I.S., Whitehouse M.J. (2019) In situ trace element and Sm-Nd isotope analysis of accessory minerals in an Eoarchean tonalitic gneiss from Greenland: Implications for Hf and Nd isotope decoupling in Earth's ancient rocks. *Chem. Geol.* 524, 394-405.
- Hammouda T., Chantel J., Devidal J.-L. (2010) Apatite solubility in carbonatitic liquids and trace element partitioning between apatite and carbonatite at high pressure. *Geochim. Cosmochim. Acta* 74, 7220-7235.
- Hasebe N., Barbarand J., Jarvis K., Carter A., Hurford A.J. (2004) Apatite fission-track chronometry using laser ablation ICP-MS. *Chem. Geol.* 207, 135-145.
- Isnard H., Brennetot R., Caussignac C., Caussignac N., Chartier F. (2005) Investigations for determination of Gd and Sm isotopic compositions in spent nuclear fuels samples by MC ICPMS. *Int. J. Mass Spectrom.* 246, 66-73.
- Košler J., Wiedenbeck M., Wirth R., Hovorka J., Sylvester P., Mikova J. (2005) Chemical and phase composition of particles produced by laser ablation of silicate glass and zircon – implications for elemental fractionation during ICP-MS analysis. *J. Anal. At. Spectrom.* 20, 402-409.
- Kuhn H.R., Günther D. (2003) Elemental Fractionation Studies in Laser Ablation Inductively Coupled Plasma Mass Spectrometry on Laser-Induced Brass Aerosols. *Anal. Chem.* 75, 747-753.

- Iizuka T., Eggins S.M., McCulloch M.T., Kinsley L.P.J., Mortimer G.E. (2011) Precise and accurate determination of 147Sm/144Nd and 143Nd/144Nd in monazite using laser ablation-MC-ICPMS. *Chem. Geol.* 282, 45-57.
- Lugmair G.W. and K. Marti (1978) Lunar Initial 143Nd/144Nd: Differential Evolution of the Lunar Crust and Mantle. *Earth Planet. Sci. Lett.* 39, 349-357.
- Lyons J.L. (1988) Volcanogenic iron oxide deposits, Cerro de Mercado and vicinity, Durango. *Econ. Geol.* 83, 1886-1906.
- Mata J., Moreira M., Doucelance R., Ader M., Silva L. C. (2010) Noble gas and carbon isotopic signatures of Cape Verde oceanic carbonatites. Implications for carbon provenance. *Earth Planet. Sci. Lett.* 291, 70–83.
- McDowell F.W., McIntosh W.C., Farley K.A. (2005) A precise 40Ar–39Ar reference age for the Durango apatite (U–Th)/He and fission-track dating standard. *Chem. Geol.* 214, 249-263.
- McFarlane C.R.M., McCulloch M.T. (2007) Coupling of in-situ Sm-Nd systematics and U-Pb dating of monazite and allanite with applications to crustal evolution studies. *Chem. Geol.* 245, 45-60.
- Mitchell R.H., Wu F.Y., Yang Y.H. (2011) In situ U-Pb, Sr and Nd isotopic analysis of loparite by LA-(MC)-ICP-MS. *Chem. Geol.* 280, 191-199.
- Newman K., freedman P.A., Williams J., Belshaw N.S., Halliday A.N. (2009) High sensitivity skimmers and non-linear mass dependent fractionation in ICP-MS. *J. Anal. At. Spectrom.* 24, 742-751.
- Newman K. (2012) Effects of the sampling interface in MC-ICP-MS: Relative elemental sensitivities and non-linear mass dependent fractionation of Nd isotopes. *J. Anal. At. Spectrom.* 27, 63-70.
- Qian S.-P., Zhang L. (2019) Simultaneous in situ determination of rare earth element concentrations and Nd isotope ratio in apatite by laser ablation ICP-MS. *Geochem. J.* 53, 319-328.
- Rankenburg K., Brandon A.D., Neal C.R. (2006) Neodymium isotope evidence for a chondritic composition of the Moon. *Science* 312, 1369-1372.
- Rønsbo J. (1989) Coupled substitutions involving REEs and Na and Si in apatites in alkaline rocks from the Ilimaussaq intrusion, South Greenland, and the petrological implications. *Am. Mineral.* 74, 896-901.
- Russell W.A., Papantastassiou D.A., Tombrello T.A. (1978) Ca isotope fractionation on the Earth and other solar system materials. *Geochim. Cosmochim. Acta* 42, 1075-1090.
- Spandler C., Hammerli J., Sha P., Hilbert-wolf H., Hu Y., Roberts E., Schmitz M. (2016) MKED1: a new titanite standard for in situ analysis of Sm–Nd isotopes and U–Pb geochronology. *Chem. Geol.* 425, 110–126.
- Thirlwall M.F. (2002) Multicollector ICP-MS analysis of Pb isotopes using a ^{207}pb-^{204}pb double spike demonstrates up to 400 ppm/amu systematic errors in Tl-normalization. *Chem. Geol.* 184, 255-279.
- Trotter J.A., Eggins S.M. (2006) Chemical systematics of conodont apatite determined by laser ablation ICPMS. *Chem. Geol.* 233, 196-216.
- Vance D., Thirlwall M. (2002) An assessment of mass discrimination in MC-ICPMS using Nd isotopes. *Chem. Geol.* 185, 227-240.
- Wasserburg G.J., Jacobsen S.B., DePaolo D.J., McCulloch M.T., Wen T. (1981) Precise determination of Sm/Nd ratios, Sm and Nd isotopic abundances in standard solutions. *Geochim. Cosmochim. Acta* 45, 2311-2323.

- Wu F.Y., Yang Y.H., Li Q.L., Mitchell R.H., Dawson J.B., Brandl G., Yuhara M. (2011) In situ determination of U-Pb ages and Sr-Nd-Hf isotopic constraints on the petrology of the Phalaborwa carbonatite complex, South Africa. *Lithos* 127, 309-322.
- Xu L., Hu Z., Zhang W., Yang L., Liu Y., Gao S., Luo T., Hu S. (2015) In situ Nd isotope analyses in geological materials with signal enhancement and non-linear mass dependent fractionation reduction using laser ablation MC-ICP-MS. *J. Anal. At. Spectrom.* 30, 232-244.
- Xu L., Yang J., Ni Q., Yang Y., Hu Z., Liu Y., Wu Y., Luo T., Hu S. (2018) Determination of Sm-Nd Isotopic Compositions in Fifteen Geological Materials Using Laser Ablation MC-ICP-MS and Application to Monazite Geochronology of Metasedimentary Rock in the North China Craton. *Geostand. Geoanalytical Res.* 42, https://doi.org/10.1111/ggr.12210.
- Yang Y.H., Sun J.F., Xie L.W., Fan H.R., Wu F.Y. (2008) In situ Nd isotopic measurement of natural geological materials by LA-MC-ICPMS. *Chin. Sci. Bull.* 53, 1062–1070.
- Yang Y.-H., Wu F.-Y., Yang J.-H., Chew D.M., Xie L.-W., Chu Z.-Y., Zhang Y.-B., Huang C. (2014) Sr and Nd isotopic compositions of apatite reference materials used in U–Th–Pb geochronology. *Chem. Geol.* 385, 35-55.
- Yuhara M., Hirahara Y., Nishi N., Kagami H. (2005) Rb–Sr, Sm–Nd ages of the Phalaborwa carbonatite complex, South Africa. *Polar Geosci.* 18, 101–113.
- Zeitler P., Herczeg A., McDougall I., Honda M. (1987) U-Th-He dating of apatite: A potential thermochronometer. *Geochim. Cosmochim. Acta* 51, 2865-2868.

Table 1

Sm/Nd chemical and isotopic characteristics of Durango crystal available at the LMV and Phalaborwa PHB09 apatites.

Sample	*[Sm] ppm*	*[Nd] ppm*	*$^{147}Sm/^{144}Nd$*	*$^{143}Nd/^{144}Nd$*	*$^{143}Nd/^{144}Nd$*
Durango 1-1 [1]	128	1020	0.0760 (±5)	0.512470 (±6)	0.348407 (±3)
Durango 1-2 [1]	128	1021	0.0760 (±5)	0.512476 (±3)	0.348414 (±2)
Durango 2	131	1038	0.0760 (±5)	0.512473 (±4)	0.348407 (±2)
Durango 3	135	1066	0.0764 (±5)	0.512475 (±3)	0.348407 (±2)
Mean Durango	*130 ± 6* [2]	*1036 ± 43* [2]	*0.0761 ± 0.0004* [2]	*0.512473 ± 0.000005* [2]	*0.348409 ± 0.000007* [2]
PhB09-1	413	2108	0.1185 (±8)	0.511274 (±4)	0.348398 (±3)
PhB09-2	415	2110	0.1189 (±8)	0.511286 (±4)	0.348394 (±3)
PhB09-3	398	2049	0.1172 (±8)	0.511261 (±4)	0.348396 (±3)
Mean PhB09	*409 ± 19* [2]	*2089 ± 69* [2]	*0.1182 ± 0.0017* [2]	*0.512473 ± 0.000025* [2]	*0.348396 ± 0.000004* [2]

[1] Sample D1 was separated into subsamples D1-1 and D1-2 after acid-digestion and addition of a ^{150}Nd-^{149}Sm spike. The good reproducibility between D1-1 and D1-2 attests to the quality of the chemical separation. [2] Uncertainty in calculated means is 2 standard deviations.

Table 2

MC-ICPMS cup configuration and potential interferences.

Faraday Cup	*L4*	*L3*	*L2*	*L1*	*Axial*	*H1*	*H2*
Main isotopes	^{143}Nd	^{144}Nd	^{145}Nd	^{146}Nd	^{147}Sm	^{148}Nd	^{149}Sm
Interferences		^{144}Sm		$^{130}Ba^{16}O$		$^{148}Sm+^{132}Ba^{16}O$	

Table 3

LA-MC-ICPMS parameters.

MC-ICPMS		*Laser ablation*	
Model	Neptune plus	Type	Excimer 193-nm M-50E
Forward power	1200 W	Model	Resonetics
Mass resolution	400	Mode	1 spot ~50 cycles
Integration time	1.094 s	Frequency	5-10 Hz
		Spot size	33-93 microns
Gas flows (l/min)		Laser fluence	3.5-5 J/cm^2
Cool / plasma	15.50	*Gas flows (ml/mn)*	
Auxiliary (Ar)	0.72	Helium	650-800
Sample (Ar)	0.974-0.984	Nitrogen	2-3.5

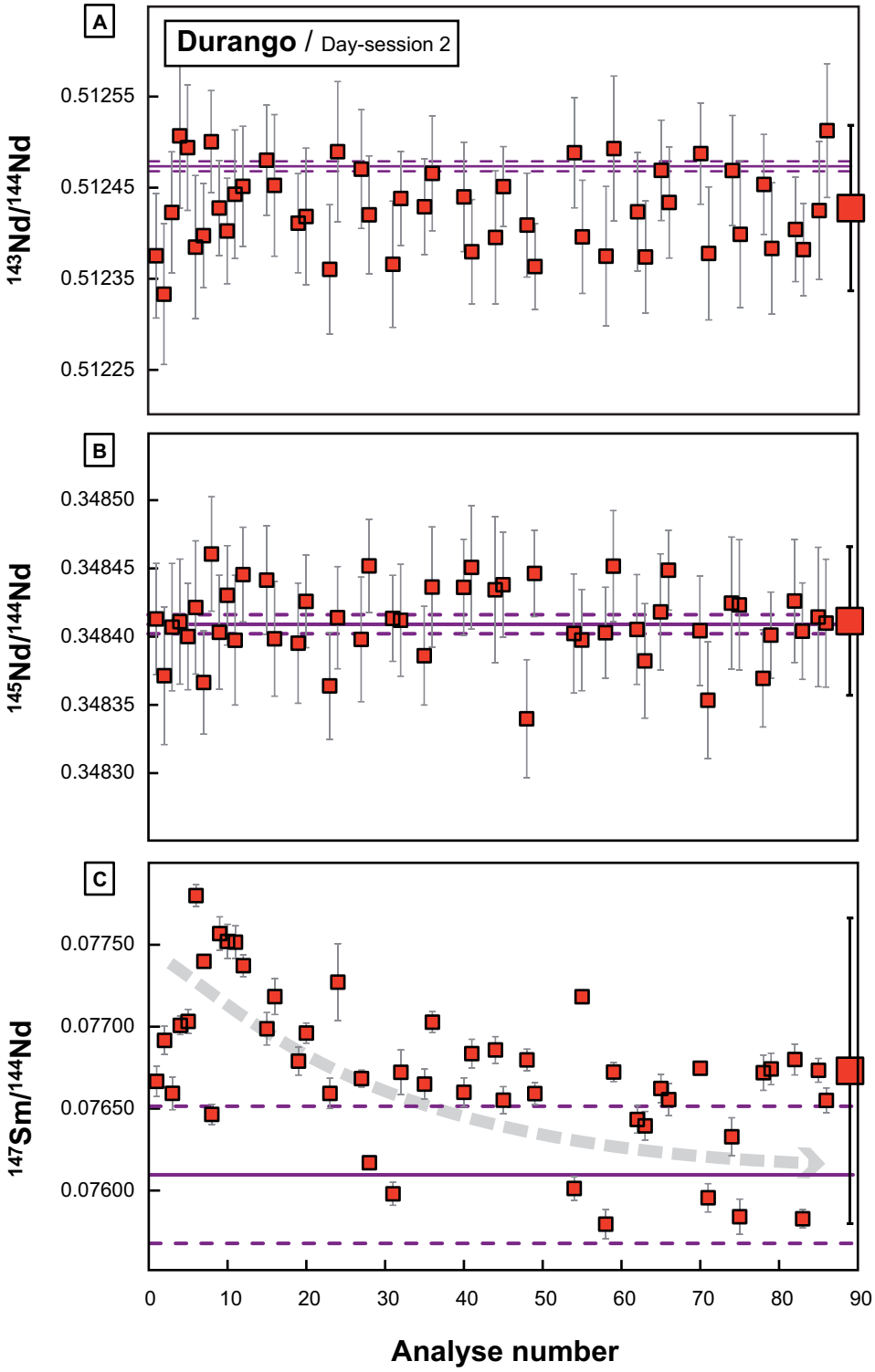

Figure 1: (A) $^{143}Nd/^{144}Nd$, (B) $^{145}Nd/^{144}Nd$, and (C) $^{147}Sm/^{144}Nd$ ratios of Durango apatite acquired during day-session 2 (measurements done for five hours) at constant laser parameters (spot size = 40 µm, fluence = 3.8 J/cm^2, and frequency = 6 Hz). The data are reported in chronological order of acquisition. Also plotted are the TIMS determinations (purple lines) ± 2 s.d. (dashed, purple lines). A slight, « instrumental » drift leading to elemental fractionation (C) cannot be excluded.

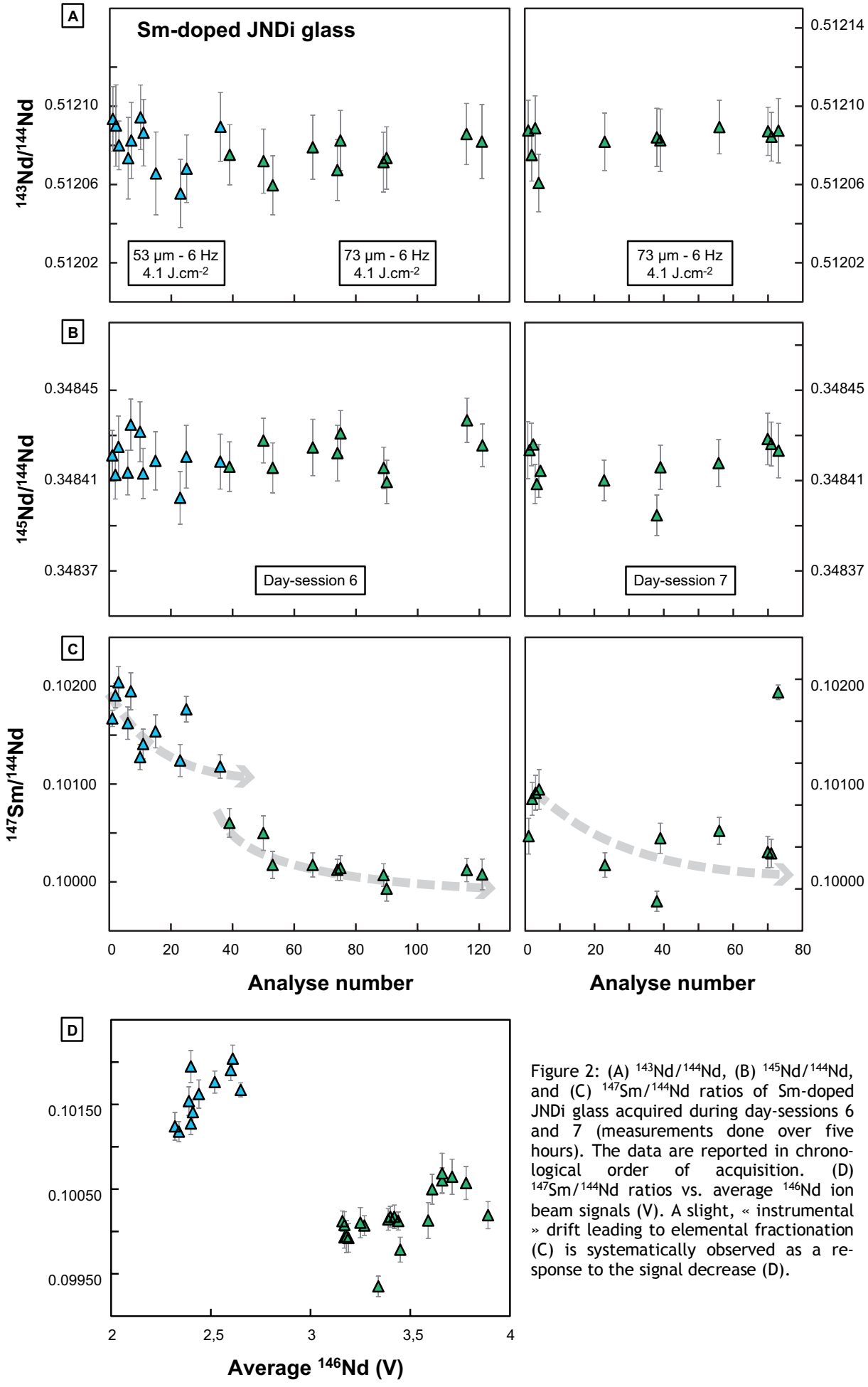

Figure 2: (A) $^{143}Nd/^{144}Nd$, (B) $^{145}Nd/^{144}Nd$, and (C) $^{147}Sm/^{144}Nd$ ratios of Sm-doped JNDi glass acquired during day-sessions 6 and 7 (measurements done over five hours). The data are reported in chronological order of acquisition. (D) $^{147}Sm/^{144}Nd$ ratios vs. average ^{146}Nd ion beam signals (V). A slight, « instrumental » drift leading to elemental fractionation (C) is systematically observed as a response to the signal decrease (D).

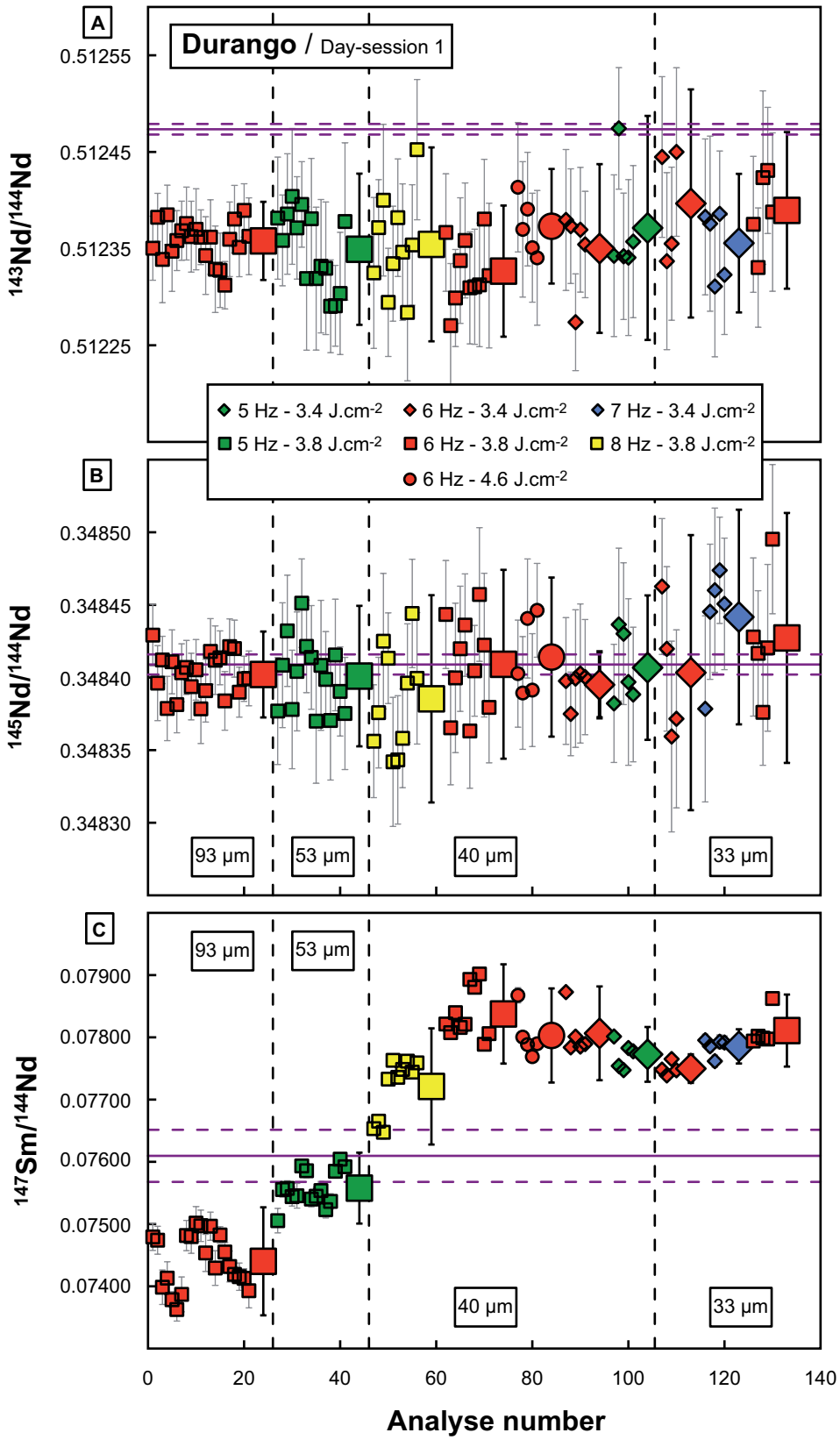

Figure 3: (A) $^{143}Nd/^{144}Nd$, (B) $^{145}Nd/^{144}Nd$, and (C) $^{147}Sm/^{144}Nd$ ratios of Durango apatite measured by LA-MC-ICPMS during day-session 1. The data are reported in chronological order of acquisition. Each symbol corresponds to a given set of frequency and fluence (see inset between A and B); values inside white rectangles refer to the size of the spot. Also reported are the TIMS determinations (purple lines) ± 2 s.d. (dashed, purple lines).

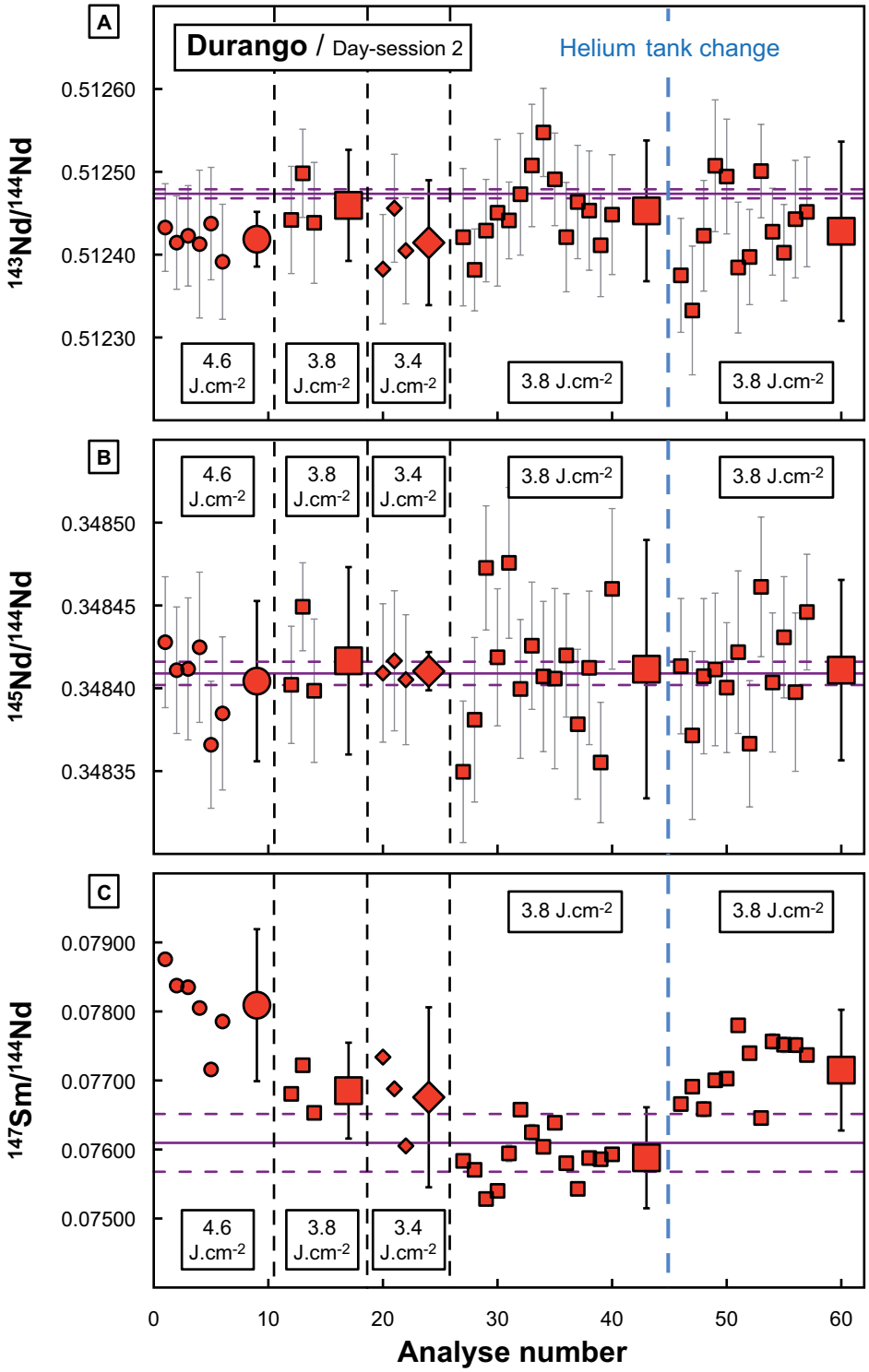

Figure 4: Effect of laser fluence on (A) $^{143}Nd/^{144}Nd$, (B) $^{145}Nd/^{144}Nd$, and (C) $^{147}Sm/^{144}Nd$ ratios of Durango apatite (spot-size = 40 µm, frequency = 6 Hz). Analyzes were performed during day-session 2. The dashed, blue line indicates when the helium tank was changed. The data are reported in chronological order of acquisition (note that the 12 runs performed after the tank change correspond to the first 12 runs reported on Figure 1). Also plotted are the TIMS determinations (purple lines) ± 2 s.d. (dashed, purple lines).

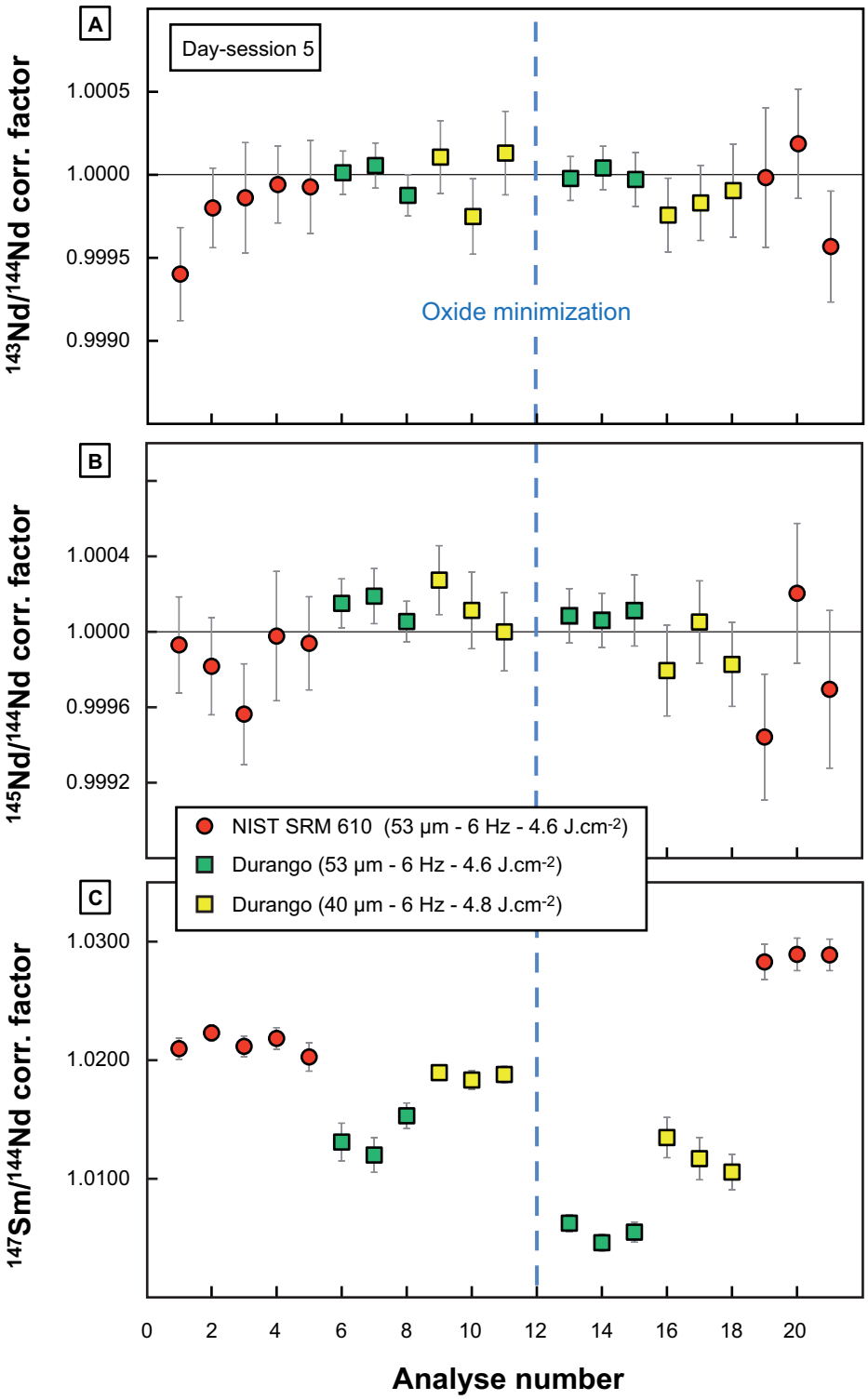

Figure 5: Effect of oxide minimization on (A) $^{143}Nd/^{144}Nd$, (B) $^{145}Nd/^{144}Nd$, and (C) $^{147}Sm/^{144}Nd$ ratios of Durango apatite and NIST SRM 610. Measurements were done with H-skimmer coupled to sampler cone. Correction factors corresponds to the ratios of measured values over reference ones. Values for NIST SRM 610 are from Yang *et al.* (2014). Analyzes were performed during day-session 5; they are reported in chronological order of acquisition. The dashed, blue line indicates when the minimization was operated.

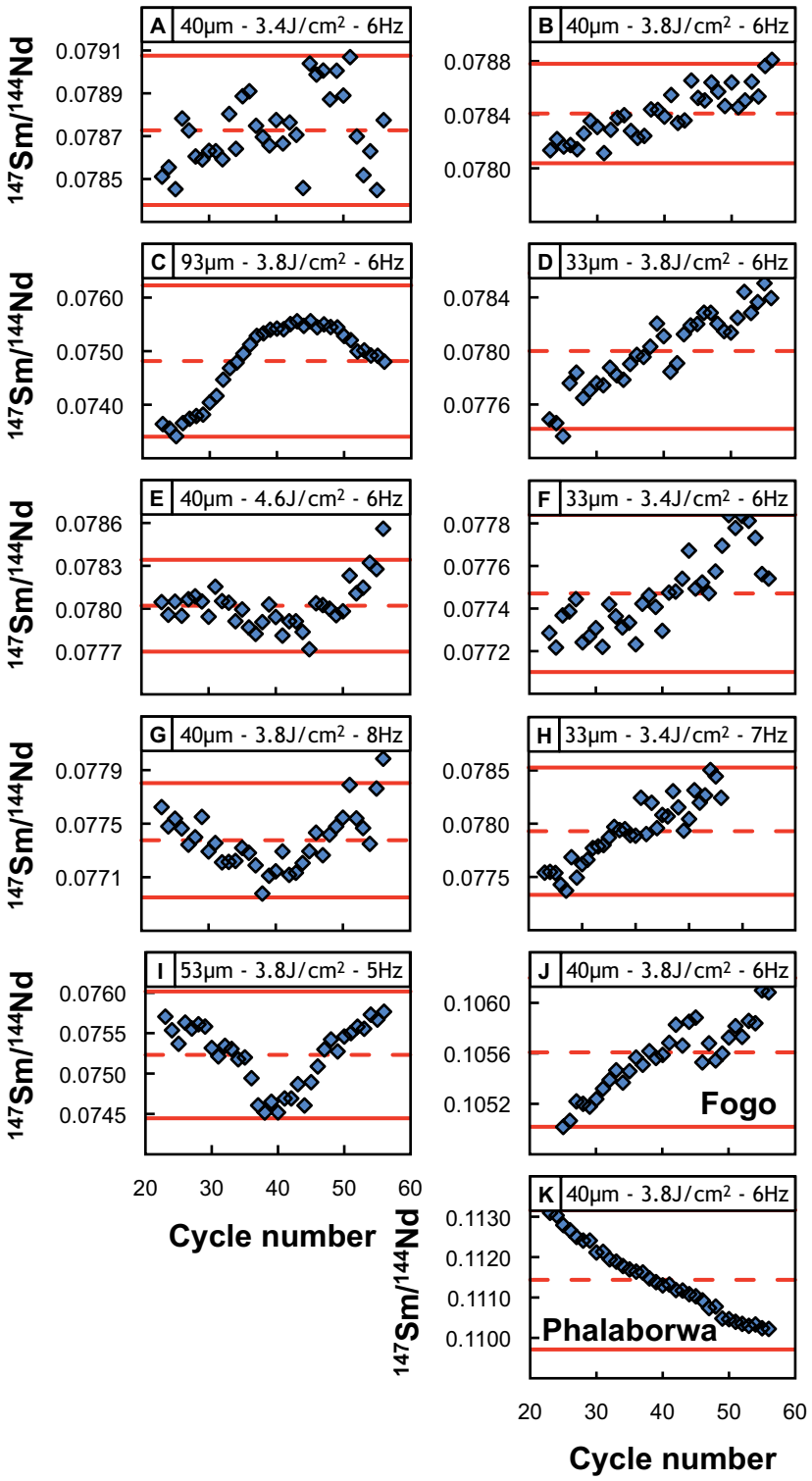

Figure 6: (A) to (K) report cycle-to-cycle $^{147}Sm/^{144}Nd$ ratios measured in Durango, Fogo and Phalaborwa apatites for different sets of laser parameters (values indicated inside white rectangles). Also plotted are the mean value (dashed, red lines) ± 2 s.d. (red lines) for each analysis. All data were acquired during successive day-sessions 1, 2 and 3.

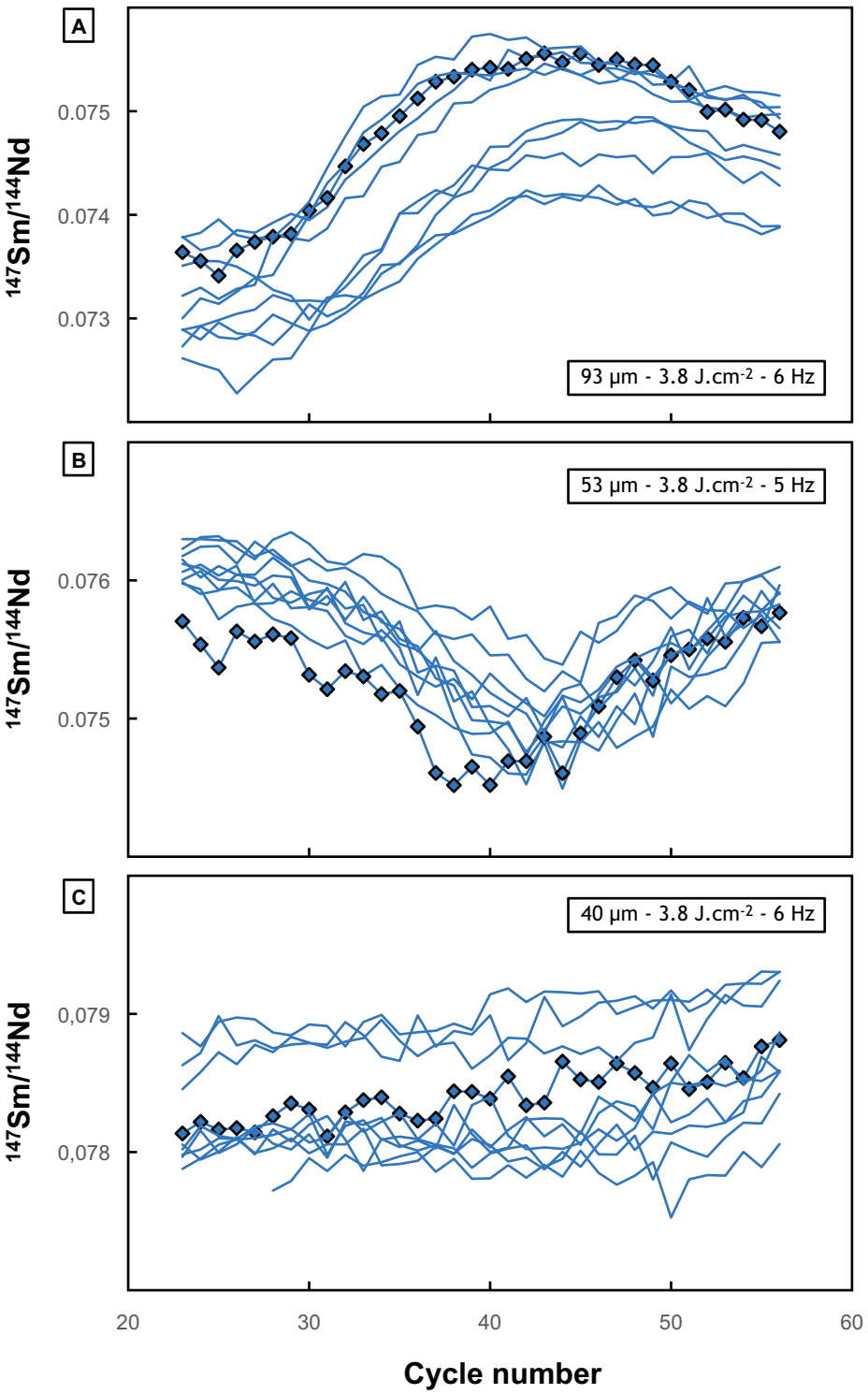

Figure 7: Reproducibility of cycle-to-cycle $^{147}Sm/^{144}Nd$ variations (10 consecutive analyzes). Values inside white rectangles give the laser parameters. Patterns with blue diamonds are those reported in figures 6C, 6I and 6B, respectively.

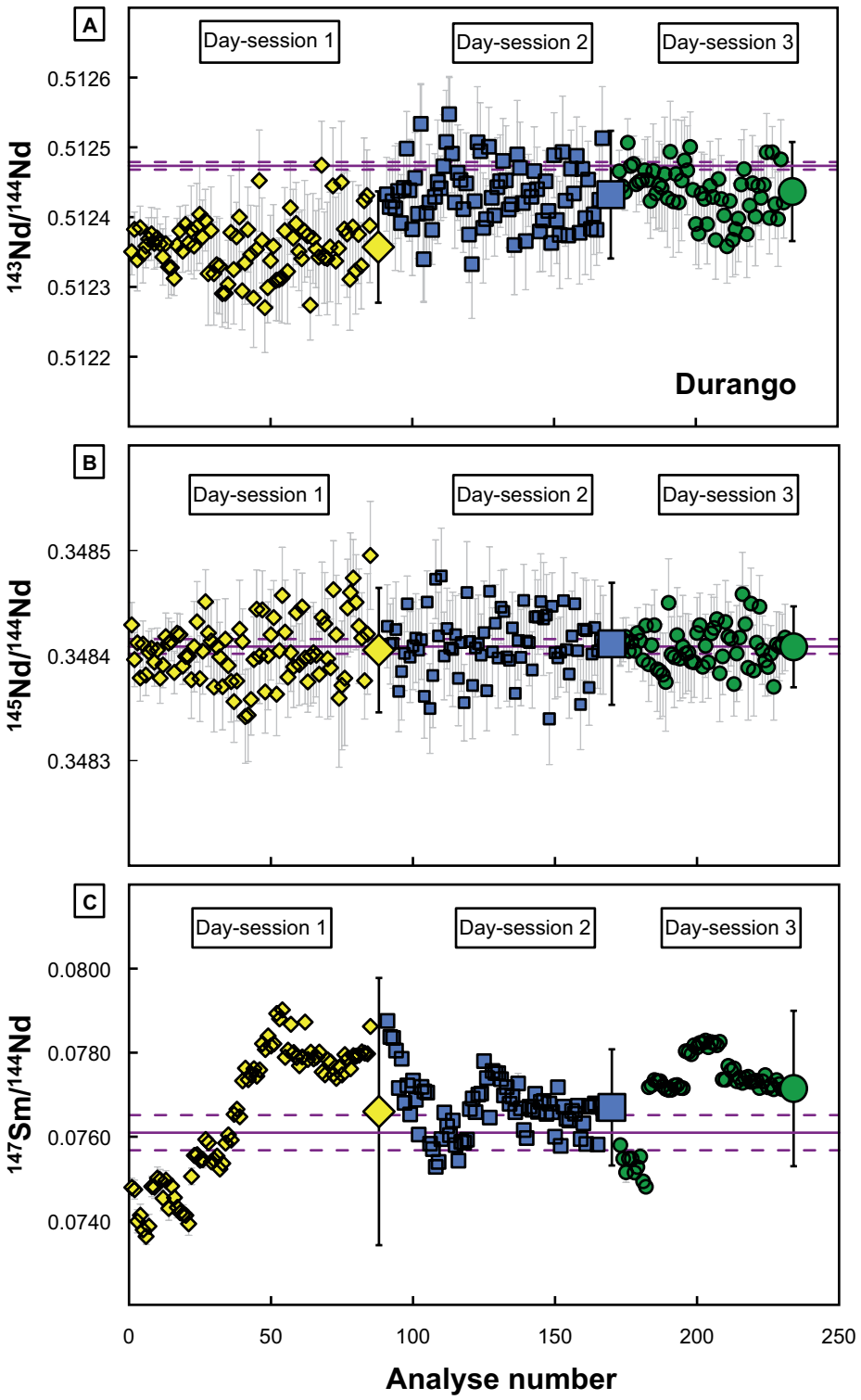

Figure 8: (A) $^{143}Nd/^{144}Nd$, (B) $^{145}Nd/^{144}Nd$, and (C) $^{147}Sm/^{144}Nd$ ratios of Durango apatite measured in the same chip during 3 day-sessions of acquisition (3 sessions over one month: 2 successive days and another one 30 days later) for various laser parameter values. The data are reported in chronological order of acquisition. Also plotted are the TIMS determinations (purple lines) ± 2 s.d. (dashed, purple lines).

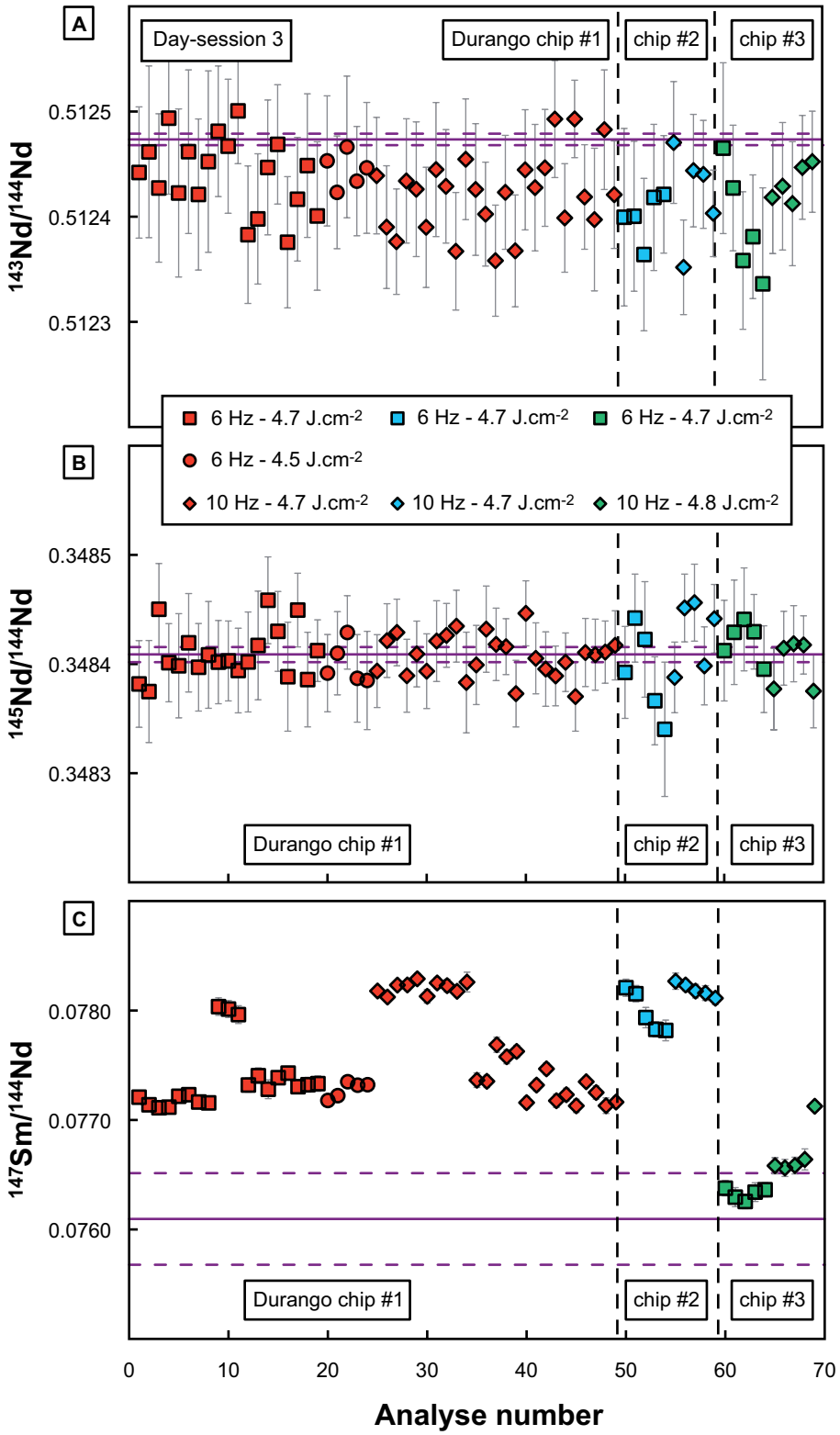

Figure 9: (A) $^{143}Nd/^{144}Nd$, (B) $^{145}Nd/^{144}Nd$, and (C) $^{147}Sm/^{144}Nd$ ratios of Durango apatite measured in three distinct chips during the third day-session (spot size = 40 µm, fluence and frequency are given in the inset). The data are reported in chronological order of acquisition. Also plotted are the TIMS determinations (purple lines) ± 2 s.d. (dashed, purple lines).

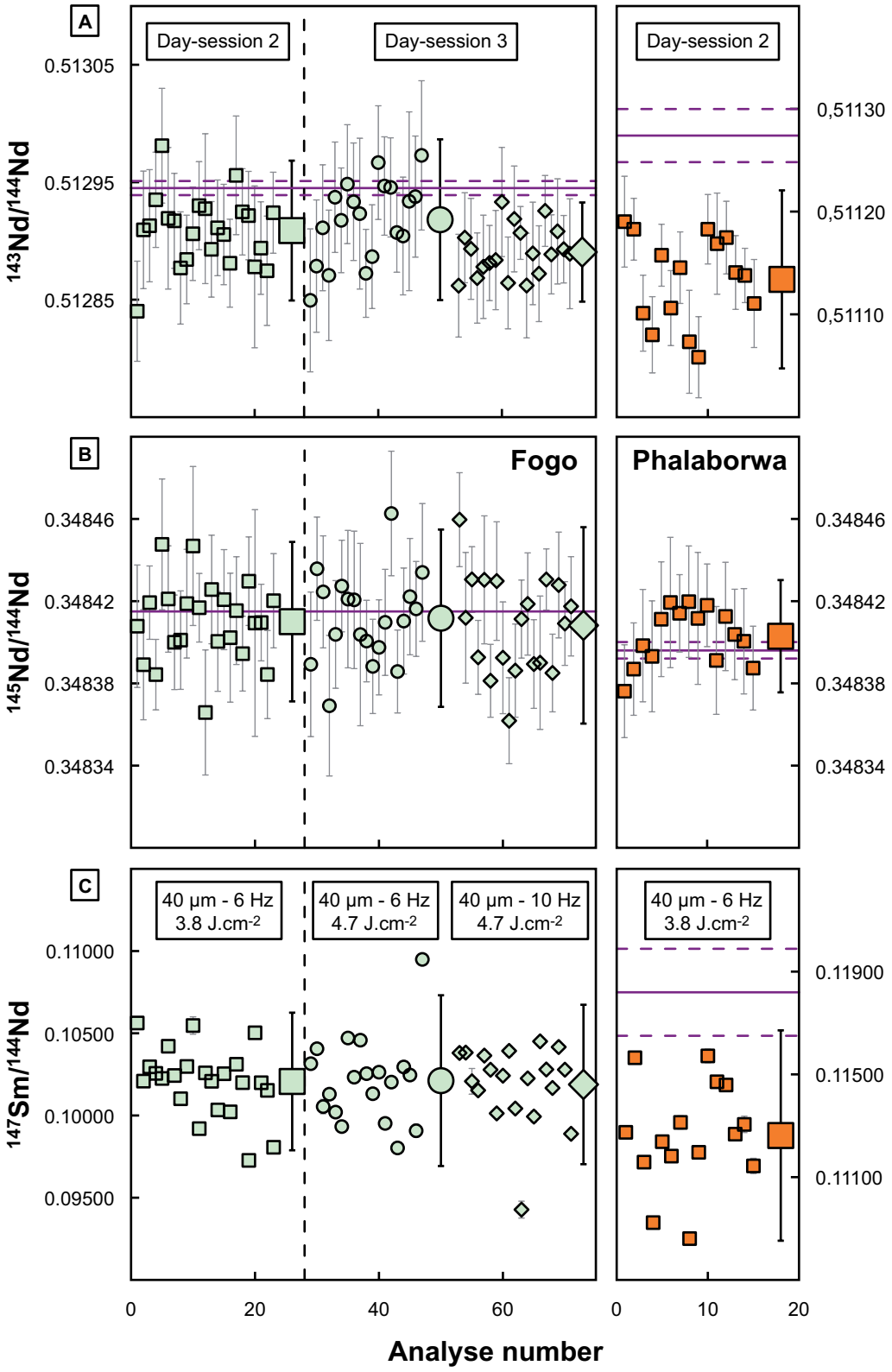

Figure 10: (A) $^{143}Nd/^{144}Nd$, (B) $^{145}Nd/^{144}Nd$, and (C) $^{147}Sm/^{144}Nd$ ratios measured in apatite grains from Fogo, Cape Verde Islands (left column), and Phalaborwa, South Africa (right column). The data are reported in chronological order of acquisition. Also plotted are the corresponding TIMS determinations (purple lines) ± 2 s.d. (dashed, purple lines). The accuracy and precision of Fogo analyzes are few dependent on the energy or the frequency of the laser.

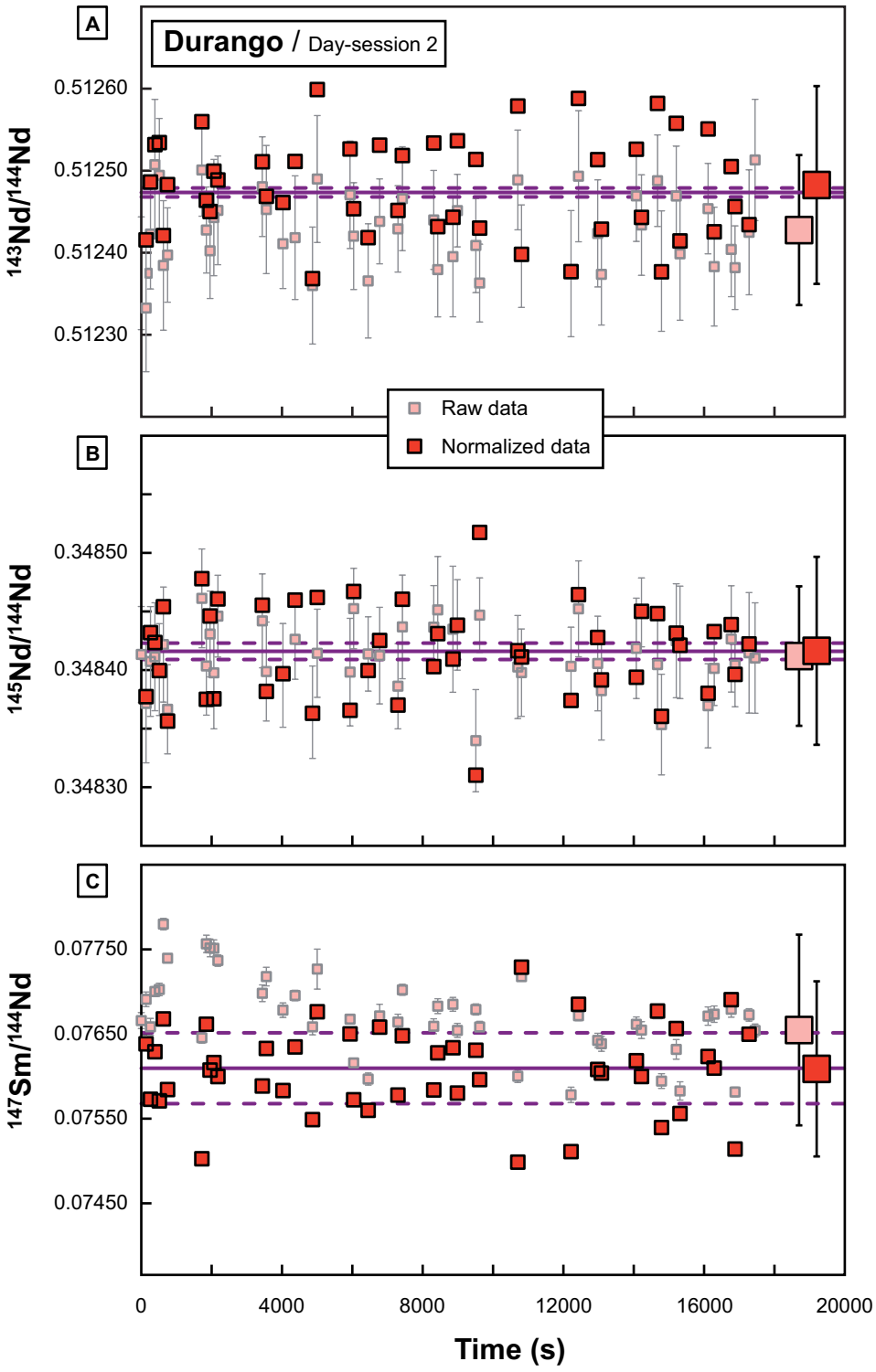

Figure 11: External normalization of (A) $^{143}Nd/^{144}Nd$, (B) $^{145}Nd/^{144}Nd$, and (C) $^{147}Sm/^{144}Nd$ ratios of Durango apatite (40 µm, 3.8 J/cm^2, 6 Hz). Each measurement (at given t) is normalized to the mean value of (t-1) and (t+1) analyzes assuming a linear, step-by-step, time-depending variation of measured ratios and TIMS determinations. Pink symbols are measured data, and red squares are normalized ones. Also plotted are the corresponding TIMS determinations (purple lines) ± 2 s.d. (dashed, purple lines).

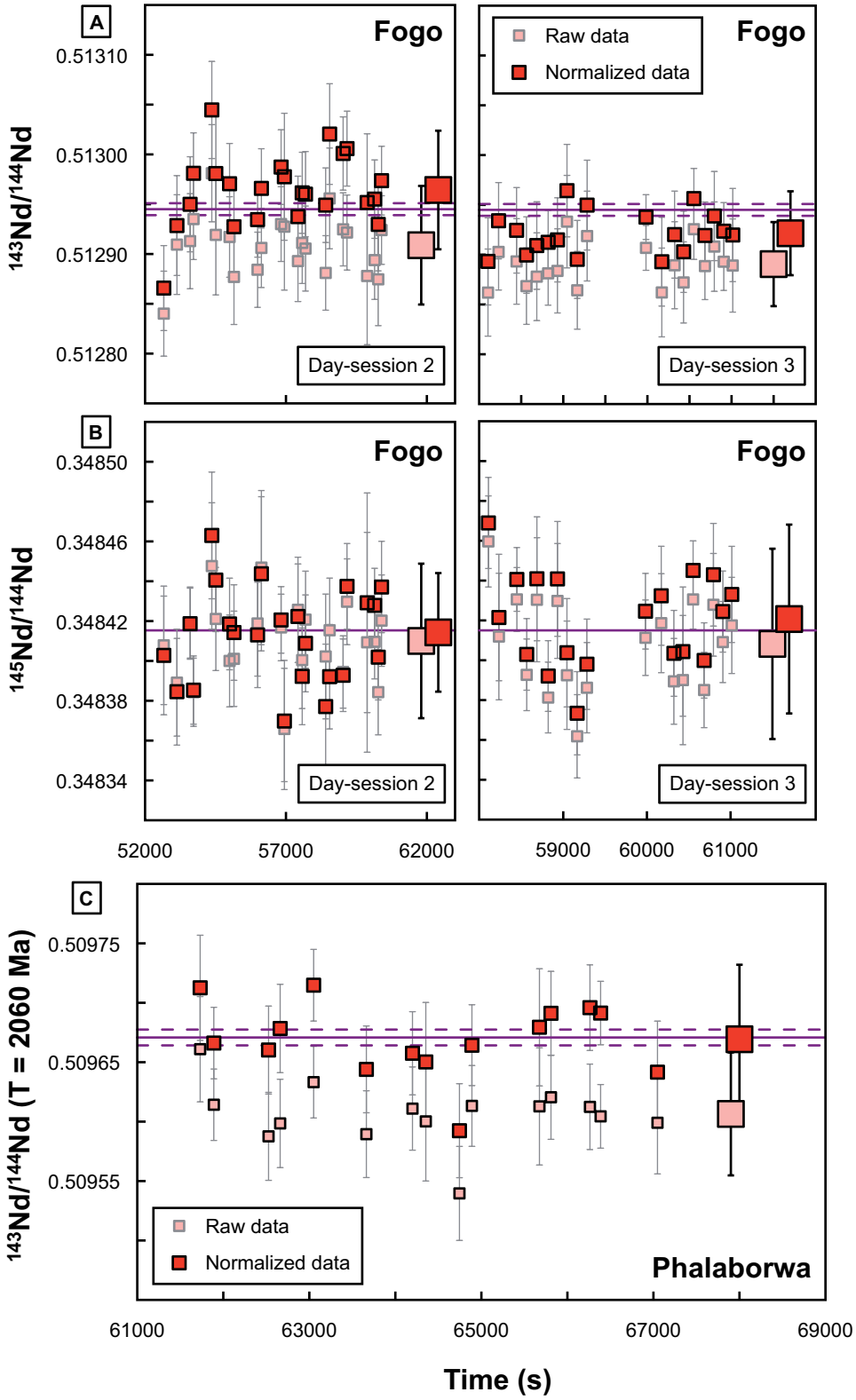

Figure 12: External normalization of (A) $^{143}Nd/^{144}Nd$ and (B) $^{145}Nd/^{144}Nd$ ratios of Fogo grains, and (C) initial $^{143}Nd/^{144}Nd$ ratios of Phalaborwa grains against Durango apatite. Pink symbols are measured data, and red squares are normalized ones. Also plotted are the corresponding TIMS determinations (purple lines) ± 2 s.d. (dashed, purple lines).

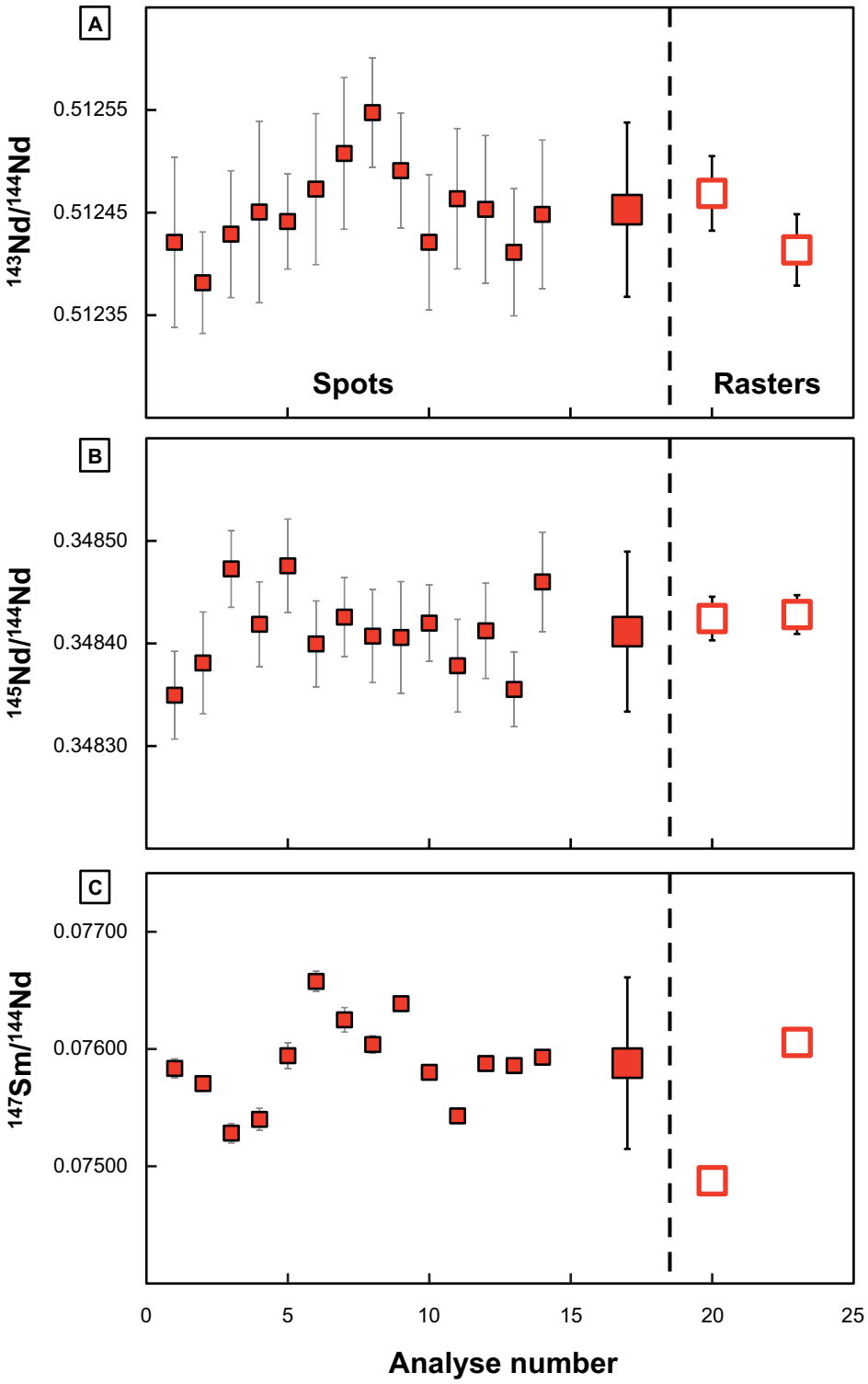

Figure 13: Comparison between raster (length ~150 µm) and spot measurements operated one after the other during day-session 2 in Durango Apatite. A) $^{143}Nd/^{144}Nd$, (B) $^{145}Nd/^{144}Nd$, and (C) $^{147}Sm/^{144}Nd$. Laser parameters are as follows: 40 µm - 3.8 J/cm^2 - 6 Hz. Within-run error-bars are divided by a factor 2-3 for each ratio.